Eur. Phys. J. C 51, 113–133 (2007)
DOI 10.1140/epjc/s10052-007-0268-9

THE EUROPEAN PHYSICAL JOURNAL C

Regular Article – Theoretical Physics

Heavy flavor hadrons in statistical hadronization of strangeness-rich QGP

I. Kuznetsova[a], J. Rafelski[b]

University of Arizona, Department of Physics, 1118E. 4th Street, Tucson, AZ 85721-0081, USA

Received: 18 July 2006 / Revised version: 9 February 2007 /
Published online: 28 March 2007 –

Abstract. We study b and c quark hadronization from QGP. We obtain the yields of charm and bottom flavored hadrons within the statistical hadronization model. The important novel feature of this study is that we take into account the high strangeness and entropy content of QGP, conserving the strangeness and entropy yields at hadronization.

PACS. 25.75.Nq; 12.38.Mh; 25.75.-q; 24.10.Pa

1 Introduction

A relatively large number of hadrons containing charm and bottom quarks are expected to be produced in heavy-ion (AA) collisions at the large hadrons collider (LHC). Because of their large mass $c, \bar{c}, b, \bar{b}$ quarks are produced predominantly in primary parton–parton collisions [1], at RHIC [2], and thus even more so at LHC. These heavy flavor quarks from the beginning participate in the evolution of the dense QCD matter. In view of the recent RHIC results one may hope that their momentum distribution could reach approximate thermalization within the dense QGP phase [3].

In our approach we will tacitly assume that the following evolution stages are present in heavy-ion collisions:

1. primary partons collide producing c, b quarks;
2. a thermalized parton state within $\tau = \tau_{\rm th} \simeq 0.25$–$1\ {\rm fm}/c$ is formed, and by the end of this stage nearly all entropy is produced;
3. subsequent chemical equilibration: diverse thermal particle production reactions occur, allowing first the approach to chemical equilibrium by gluons g and light non-strange quarks $q = u, d$;
4. strangeness chemical equilibration within $\tau \sim 5\ {\rm fm}/c$;
5. hadronization to the final state in about $\tau \sim 10\ {\rm fm}/c$.

It is important to observe that, in the presence of a deconfined QGP phase, heavy hadrons containing more than one heavy quark are made from heavy quarks created in different initial NN collisions. Therefore, the yields of these hadrons are expected to be enhanced as compared to the yields seen in single NN collisions [4, 5]. We note that the $B_c(b\bar{c}, \bar{b}c)$ and $J/\Psi(c\bar{c})$ and more generally all bound $c\bar{c}$ states yields were calculated before in kinetic formation and dissociation models [4, 6]. Our present work suggests that it is important to account for the binding of heavy flavor with strangeness, an effect that depletes the eligible supply of heavy flavor quarks that could form $B_c(b\bar{c}, \bar{b}c)$ and $J/\Psi(c\bar{c})$ [7].

An enhanced production yield of multi-heavy hadrons can be considered to be an indicator of the presence of deconfined QGP phase for reasons that are analogous to those of the case of multi-strange (anti-) baryons [8]. Considering that we have little doubt that QGP is the state of matter formed in the very high energy AA interactions, the study of the yields of multi-heavy hadrons is primarily explored in this work in order to falsify, or justify, the features of the statistical hadronization model (SHM) employed or the model itself in the context of the formation of heavy flavor hadrons.

For example, different from other recent studies, which assume that the hadron yields after hadronization are in chemical equilibrium [5, 9], we form the yields based on an abundance of u, d, s quark pairs, as these are available at the chemical freeze-out (particle formation) conditions in the quark–gluon phase. This approach is justified by the expectation that in a fast break-up of the QGP formed at RHIC and LHC the phase entropy and strangeness will be nearly conserved during the process of hadronization. We will investigate in quantitative terms how such chemical non-equilibrium yields, in the conditions we explore, well above the chemical equilibrium abundance, influence the expected yields of single- and multi-heavy flavor hadrons.

In the order to evaluate the yields of the final state hadrons, we enforce conservation of entropy and of the flavor s, c, b quark pair number during the phase transition or transformation. The faster the transition, the less likely

[a] e-mail: kouznet@physics.arizona.edu
[b] e-mail: rafelski@physics.arizona.edu

it is that there is a significant change in the strange quark pair yield. Similarly, any entropy production is minimized when the entropy-rich QGP break-up into the entropy-poor HG occurs rapidly. The entropy conservation constraint fixes the final light quark yield. We assume a fast transition between the QGP and HG phases, such that all hadron yields are under the same physical conditions as in QGP break-up.

In the evaluation of the heavy particle yields we form ratios involving as normalizer the total heavy flavor yield, and for the yields of particles with two heavy quarks we use as normalizer the product of the total yields of the corresponding heavy flavors so that the results that we will consider are as little as possible dependent on the unknown total yield of charm and bottom at RHIC and LHC. The order of magnitude of the remaining dependence on heavy flavor yield is set by the ratio of the yield of all particles with two heavy quarks to the yield of particles with one heavy quark. This ratio depends on the density of heavy flavor at hadronization, $(\mathrm{d}N_c/\mathrm{d}y)/(\mathrm{d}V/\mathrm{d}y)$. The results we present for LHC are obtained for an assumed charm and bottom quark multiplicity of

$$\frac{\mathrm{d}N_c}{\mathrm{d}y} \equiv c = 10\,, \tag{1}$$

$$\frac{\mathrm{d}N_b}{\mathrm{d}y} \equiv b = 1\,, \tag{2}$$

and $\mathrm{d}V/\mathrm{d}y = 800\,\mathrm{fm}^3$ at $T = 200\,\mathrm{MeV}$. The theoretical cross sections of the c and b quark production for RHIC and LHC can be found in [10, 11]. In certain situations, we will explore how a variation of the baseline yields (1) and (2) have an impact on the results. In particular, among the yields of multi-heavy hadrons, this influence can be noticeable; see discussion in the end of Sect. 6.1. We note that the number of b quarks cannot change during expansion, because of the large mass $m_b \gg T$. It is nearly certain that all charm in QGP at RHIC is produced in the first parton collisions; for further discussion of LHC see [12]. It appears that for all practical purposes also in the more extreme thermal conditions at LHC charm is produced in the initial parton interactions.

In order to form a physical intuition about the prevailing conditions in the QGP phase at the time of hadronization, we also evaluate the heavy quark chemical reference density, that is, the magnitude of the chemical occupancy factor in QGP, considering the pre-established initial yields of c and b from the parton collision. For this purpose we use in the deconfined QGP phase:

$$m_c = 1.2\,\mathrm{GeV}\,,$$
$$m_b = 4.2\,\mathrm{GeV}\,.$$

We also take $\lambda_i = 1, i = u, d, s$ for all light flavors, since the deviation from the particle–antiparticle yield symmetry is rather small and is immaterial in the present discussion.

When computing the yields of charm (and bottom) mesons we will distinguish only strange and non-strange abundances, but not charged with non-charged (e.g. $D^-(\bar{c}d)$ with $\overline{D}^0(\bar{c}u)$) abundances. We assume that the experimental groups that report results, depending on which types of D meson were observed, can infer the total yield (charged plus non-charged) that we present. We treat in a similar way the other heavy hadrons, always focusing on the heavy and the strange flavor content, and not distinguishing the light flavor content.

Our paper is organized as follows: we first introduce the elements of the SHM that we use to evaluate the heavy flavor hadron yields in Sect. 2. This allows us to discuss the relative yields of the strange and non-strange heavy mesons in Sect. 3, and we show how this result mutually relates the values of the strangeness chemical (non-) equilibrium parameters. In this context, we also propose a multi-particle ratio as a measure of the hadronization temperature, and explore how a multi-temperature staged freeze-out would have an impact on the relevant results.

Before proceeding to obtain the main results of this work, we introduce the notion of the conservation of entropy in Sect. 4 and of strangeness in Sect. 5, which are expected to be valid in the fast hadronization process at LHC, and we discuss how this affects the SHM statistical parameters. We consider the entropy in a system with evolving strangeness in Sect. 4.2 and show that the number of active degrees of freedom in a QGP is nearly constant. Another highlight is the discussion of sudden hadronization of strangeness and the associated values of the hadron phase space parameters in Sect. 5.4. Throughout this paper we will use explicitly and implicitly the properties of the QGP fireball and hadron phase space regarding entropy and strangeness content developed in these two sections, Sects. 4 and 5.

We now turn to a discussion of the heavy flavor hadron yields for given bulk QGP constraints in Sect. 6, where we also compare, when appropriate, to the strangeness and light quarks chemical equilibrium results. We begin with a study of the charm and bottom quark phase space occupancy parameters (Sect. 6.1) and turn in Sect. 6.2 to a discussion of the yields of single heavy mesons, which we follow up with a discussion of the yields of single heavy baryons in Sect. 6.3. Finally, in Sect. 6.4 we present the expected yields of the multi-heavy hadrons, in so far these can be considered in the grand canonical approach. We conclude our work with a brief summary in Sect. 7.

2 Statistical hadronization model

The statistical hadronization model arises from the Fermi multi-particle production model [13]. Fermi considered all hadron production matrix elements to be saturated to unity. This allows one to use the Fermi golden rule with the N-particle phase space to obtain the relative particle yields. In modern language this is SHM in micro canonical ensemble; micro canonical implies that the discrete (flavor) quantum numbers and the energy are conserved exactly.

The transition from micro canonical to canonical and to grand canonical ensembles simplifies the computational effort considerably [14]. This important step does not in our context introduce the hadron phase, although before the understanding of QGP this of course was the

reaction picture: a highly compressed hadron gas matter evaporates particles. Today, it is highly compressed hot quark–gluon matter that evaporates particles. In principle, there is no necessity to introduce a hadron gas phase of matter in order to use SHM to describe the particle production.

On the other hand, in order to understand the physical meaning of the parameters introduced to describe the hadron phase space in grand canonical ensemble, such as the temperature T, it is quite convenient to *imagine* the existence of the hadron phase that follows the QGP phase. This can be taken to the extreme, and a long lasting, chemically equilibrating phase of hadrons can be assumed that follows in time the formation of the QGP fireball. Such a reaction picture may not agree with the fast evolving circumstances of a heavy-ion collision. One should note that the study of hot hadron matter on the lattice within the realm of L-QCD involves at all times a fully equilibrated system. This will differ in key features from the non-equilibrium QGP properties accompanying the hadronization process.

The important parameters of the SHM that control the relative yields of particles are the particle specific fugacity factor λ and the space occupancy factor γ. The fugacity is related to the chemical potential: $\mu = T\ln\lambda$. The occupancy γ is, nearly, equal to the ratio of produced particles to the number of particles expected in chemical equilibrium. The actual momentum distribution is

$$\frac{\mathrm{d}^6N}{\mathrm{d}^3p\mathrm{d}^3x} \equiv f(p) = \frac{g}{(2\pi)^3}\frac{1}{\gamma^{-1}\lambda^{-1}\mathrm{e}^{E/T}\pm 1} \to \gamma\lambda\mathrm{e}^{-E/T}\,, \tag{3}$$

where the Boltzmann limit of the Fermi '(+)' and Bose '(−)' distributions is indicated; g is the degeneracy factor, T is the temperature, and $E = E(p)$ is the energy.

The fugacity λ is associated with a conserved quantum number, such as net baryon number, net strangeness, and heavy flavor. Thus the antiparticles have inverse values of λ, and the λ evolution during the reaction process is related to the changes in densities due to the dynamics, such as expansion. γ is the same for particles and antiparticles. Its value changes as a function of time even if the system does not expand, for it describes the build-up of the particular particle species. For this reason γ changes rapidly during the reaction, while λ is more constant. Thus, it is γ that carries information about the time history of the reaction and the precise conditions of particle production referred to as chemical freeze-out.

The number of particles of type i with mass m_i per unit of rapidity is in our approach given by

$$\frac{\mathrm{d}N_i}{\mathrm{d}y} = \gamma_i n_i^{\mathrm{eq}}\frac{\mathrm{d}V}{\mathrm{d}y}\,. \tag{4}$$

Here $\mathrm{d}V/\mathrm{d}y$ is the volume of the system associated with the unit of rapidity, and n_i^{eq} is a Boltzmann particle density in chemical equilibrium:

$$\begin{aligned} n_i^{\mathrm{eq}} &= g_i\int\frac{\mathrm{d}^3p}{(2\pi)^3}\lambda_i\exp(-\sqrt{p^2+m_i^2}/T) \\ &= \lambda_i\frac{T^3}{2\pi^2}g_iW(m_i/T)\,, \end{aligned} \tag{5}$$

and

$$W(x) = x^2K_2(x) \to 2 \quad \text{for} \quad x\to 0\,. \tag{6}$$

Both $m_ic^2 \to m_i$ and $kT \to T$ are measured in energy units where $\hbar, c, k \to 1$.

For the case of heavy flavors, $m \gg T$, the dominant contribution to the Boltzmann integral (5) arises from $p \simeq \sqrt{2mT}$, but we do not probe the tails of the momentum distribution. Thus, even when the momentum distribution is not well thermalized, the yield of heavy flavor hadrons can be described in terms of the thermal yields, (4), where

$$\begin{aligned} n_i^{\mathrm{eq}} = {} & \frac{g_iT^3}{2\pi^2}\lambda_i\sqrt{\frac{\pi m_i^3}{2T^3}}\exp(-m_i/T) \\ & \times\left(1+\frac{15T}{8m_i}+\frac{105}{128}\left(\frac{T}{m_i}\right)^2\dots\right). \end{aligned} \tag{7}$$

Often one can use the first term alone for the heavy flavor hadrons, since $T/m \ll 1$; however, the asymptotic series in (7) has limited validity. Our computations are all based on the CERN recursive subroutine evaluation of the Bessel functions K_2.

We use the occupancy factors γ_i^{Q} and γ_i^{H} for QGP and hadronic gas phase, respectively, tracking every quark flavor ($i = q, s, b, c$). We assume that in the QGP phase, the light quarks and gluons are adjusting fast to the ambient conditions and thus are in chemical equilibrium with $\gamma_{q,G}^{\mathrm{Q}} \to 1$. For heavy and strange flavor, the value of γ_i^{Q} under hadronization conditions is given by the number of particles present, generated by the prior kinetic processes; see (4).

The yields of different quark flavors originate in different physical processes, such as the production in the initial collisions for c, b, s, and for s also the production in thermal plasma processes. In general, we thus cannot expect that $\gamma_{c,b}^{\mathrm{Q}}$ will be near unity at hadronization. However, the thermal strangeness production process $GG \to s\bar{s}$ can nearly chemically equilibrate the strangeness flavor in plasma formed at RHIC and/or LHC [12], and we will always consider, among other cases, the limit $\gamma_s^{\mathrm{Q}} \to 1$ prior to hadronization.

The yields of all hadrons after hadronization are also given by (4), which helps us to obtain γ_i^{H} for the hadrons. In general, the evaluation of the hadron chemical parameters presents a more complicated case, since they are composed from those of the valence quarks in the hadron (three quarks, or a quark and antiquark). Therefore, in the coalescence picture, the phase space occupancy γ^{H} of the hadrons will be the product of the γ^{H} for each constituent quark. For example, for the charm meson D ($c\bar{q}$)

$$\gamma_D^{\mathrm{H}} = \gamma_c^{\mathrm{H}}\gamma_q^{\mathrm{H}}\,. \tag{8}$$

To evaluate the yields of the final state hadrons, we enforce conservation of entropy and of the flavor s, c, b quark

pair number during the phase transition or transformation. The faster the transition, the less likely it is that there will be a significant change in the strange quark pair yield. Similarly, any entropy production is minimized when the entropy-rich QGP break-up into the entropy-poor HG occurs rapidly. The entropy conservation constraint fixes the final light quark yield. We assume a fast transition between the QGP and HG phases, such that all hadron yields are under the same physical conditions as in QGP break-up.

Assuming that in the hadronization process the number of b, c, s quark pairs does not change, the three unknown quantities $\gamma_s^{\rm H}$, $\gamma_c^{\rm H}$ and $\gamma_b^{\rm H}$ can be determined from their values in the QGP phase, $\gamma_s^{\rm Q}$, $\gamma_c^{\rm Q}$ and $\gamma_b^{\rm Q}$ (or ${\rm d}N_i^{\rm Q}/{\rm d}y$) and the three flavor conservation equations,

$$\frac{{\rm d}N_i^{\rm H}}{{\rm d}y} = \frac{{\rm d}N_i^{\rm Q}}{{\rm d}y} = \frac{{\rm d}N_i}{{\rm d}y}, \quad i = s, c, b\,. \tag{9}$$

In order to conserve entropy, we have

$$\frac{{\rm d}S^{\rm H}}{{\rm d}y} = \frac{{\rm d}S^{\rm Q}}{{\rm d}y} = \frac{{\rm d}S}{{\rm d}y}\,, \tag{10}$$

where a value $\gamma_q^{\rm H} \neq 1$ is nearly always required when in the QGP phase we have $\gamma_{q,G}^{\rm Q} = 1$. This implies that the yields of hadrons with light quark content are, in general, not in chemical equilibrium, unless there is some extraordinary circumstance allowing for a prolonged period of time in which hadron reactions can occur after hadronization. Chemical non-equilibrium thus will influence the yields of heavy flavored particles in the final state as we shall discuss in this work.

As noted at the beginning of this section, the use of the hadron phase space (denoted by H above) does not imply the presence of a real physical 'hadron matter' phase: the SHM particle yields will be attained solely on the basis of the availability of this phase space, as noted at the beginning of this section. Another way to argue this is to imagine a pot of quark matter with hadrons evaporating . Which kind of hadron emerges, and at which momentum, is entirely determined by the access to the phase space, and there are only free-streaming particles in the final state.

Thinking in these terms, one can imagine that especially for heavy quark hadrons some particles are preformed in the deconfined plasma, and thus the heavy hadron yields may be based on a value of temperature which is higher than the global value expected for the other hadrons. For this reason we will study in this work the range $140 < T < 260\,{\rm MeV}$ and also consider the sensitivity to this type of two-temperature chemical freeze-out of certain heavy hadron yield ratios.

3 Relative charm hadron yields

3.1 Determination of γ_s/γ_q

We have seen, considering s/S and also s and S individually, across the phase limit, that in general one would expect chemical non-equilibrium in hadronization of chemically equilibrated QGP. We first show that this result matters for the relative charm meson yield ratio D_s/D, where $D_s(c\bar{s})$ comprises all mesons of type $(c\bar{s})$, which are listed in the bottom section of Table 1, and where the $D(c\bar{q})$ comprise the yields of all $(c\bar{q})$ states listed in the top section of Table 1. This ratio is formed based on the assumption that on the time scale of the strong interactions the family of strange charm mesons can be distinguished from the family of non-strange charm mesons.

Table 1. Open charm, and bottom, hadron states we considered. States in parenthesis either need confirmation or have not been observed experimentally, in which case we follow the values of [15, 33, 34]. We implemented charm–bottom symmetry required for certain observables. Top section: D, B mesons, bottom section: D_s, B_s mesons

Hadron	M [GeV]	$Q: c, b$	Hadron	M [GeV]	g
$D^0(0^-)$	1.8646	$Q\bar{u}$	$B^0(0^-)$	5.279	1
$D^+(0^-)$	1.8694	$Q\bar{d}$	$B^+(0^-)$	5.279	1
$D^{*0}(1^-)$	2.0067	$Q\bar{u}$	$B^{*0}(1^-)$	5.325	3
$D^{*+}(1^-)$	2.0100	$Q\bar{d}$	$B^{*+}(1^-)$	5.325	3
$D^0(0^+)$	2.352	$Q\bar{u}$	$B^0(0^+)$	5.697	1
$D^+(0^+)$	2.403	$Q\bar{d}$	$B^+(0^+)$	5.697	1
$D_1^{*0}(1^+)$	2.4222	$Q\bar{u}$	$B_1^{*0}(1^+)$	5.720	3
$D_1^{*+}(1^+)$	2.4222	$Q\bar{d}$	$B_1^{*+}(1^+)$	5.720	3
$D_2^{*0}(2^+)$	2.4589	$Q\bar{u}$	$B_2^{*0}(2^-)$	(5.730)	5
$D_2^{*+}(2^+)$	2.4590	$Q\bar{d}$	$B_2^{*+}(2^+)$	(5.730)	5
$D_s^+(0^-)$	1.9868	$Q\bar{s}$	$B_s^0(0^-)$	5.3696	1
$D_s^{*+}(1^-)$	2.112	$Q\bar{s}$	$B_s^{*0}(1^-)$	5.416	3
$D_{sJ}^{*+}(0^+)$	2.317	$Q\bar{s}$	$B_{sJ}^{*0}(0^+)$	(5.716)	1
$D_{sJ}^{*+}(1^+)$	2.4593	$Q\bar{s}$	$B_{sJ}^{*0}(1^+)$	(5.760)	3
$D_{sJ}^{*+}(2^+)$	2.573	$Q\bar{s}$	$B_{sJ}^{*0}(2^+)$	(5.850)	5

The yield ratio D_s/D calculated using (4) and (5) is shown in Fig. 1. Using (7), we see that this ratio is proportional to $\gamma_s^{\rm H}/\gamma_q^{\rm H}$ and weakly dependent on T:

$$\frac{D_s}{D} \approx \frac{\gamma_s^{\rm H}}{\gamma_q^{\rm H}} \frac{\Sigma_i g_{Ds\,i} m_{Ds\,i}^{3/2} \exp(-m_{Ds\,i}/T)}{\Sigma_i g_{Di} m_{Di}^{3/2} \exp(-m_{Di}/T)} = f(T)\frac{\gamma_s^{\rm H}}{\gamma_q^{\rm H}}\,. \tag{11}$$

A deviation of γ_s/γ_q from unity in the range that we will see in Sect. 5.4 leads to a noticeable difference in the ratio D_s/D. We show in Fig. 1 results for $T = 140, 160, 180\,{\rm MeV}$. In this T-domain, the effect due to $\gamma_s^{\rm H}/\gamma_q^{\rm H} \neq 1$ is the dominant contribution to the variation of this relative yield.

3.2 Check of statistical hadronization model

We next construct a heavy flavor particle ratio that depends on the hadronization temperature only. To cancel the fugacities and the volume we consider the ratio $J/\Psi\phi/D_s\overline{D_s}$ in Fig. 2. Here the J/Ψ yield includes the yield of the $(c\bar{c})$ mesons decaying into the J/Ψ. All phase space occupancies cancel, since $J/\Psi \propto {\gamma_c^{\rm H}}^2$, $\phi \propto {\gamma_s^{\rm H}}^2$ and $D_s \propto \gamma_c^{\rm H}\gamma_s^{\rm H}$, and similarly $\overline{D_s} \propto \gamma_c^{\rm H}\gamma_s^{\rm H}$. When here we use

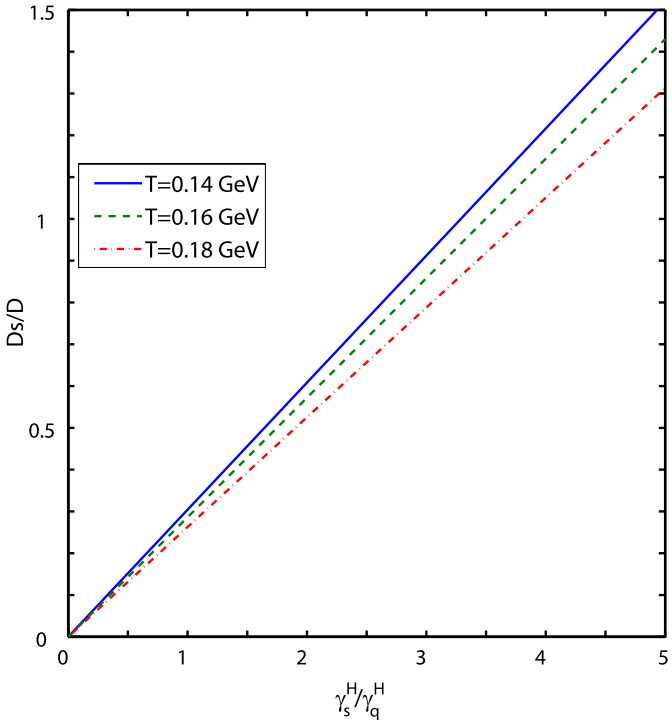

Fig. 1. The ratio D/D_s as a function of $\gamma_s^{\rm H}/\gamma_q^{\rm H}$ for $T = 140$ MeV (*blue, solid line*), $T = 160$ MeV (*green, dashed line*) and $T = 180$ MeV (*red, dash-dot line*)

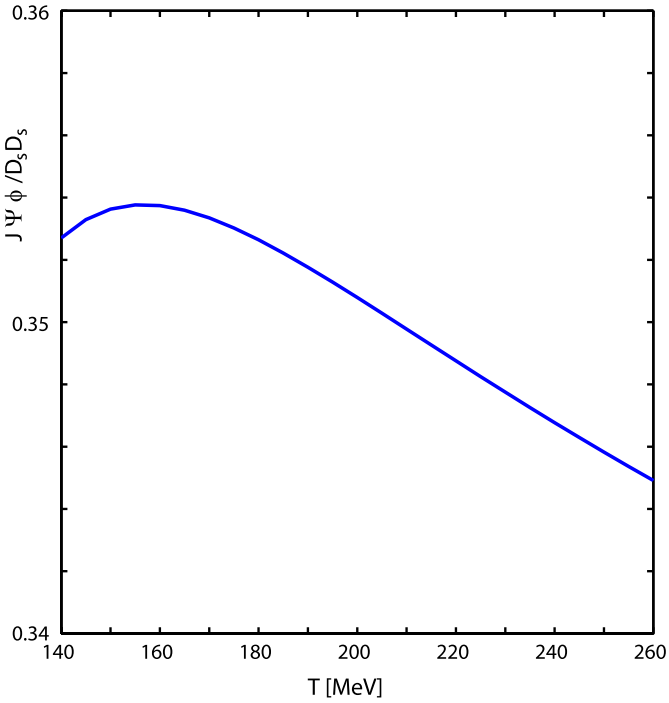

Fig. 2. The ratio $J/\Psi\phi/D_s\overline{D_s}$ as a function of the hadronization temperature T

the particle $D_s(\bar{c}s)$ and the antiparticle $\overline{D_s}(c\bar{s})$, any chemical potentials present are canceled as well. However, for the LHC and even for the RHIC environment this refinement is immaterial.

This ratio $J/\Psi\phi/D_s\overline{D_s}$, turns out to be practically constant, within a rather wide range of hadronization temperatures T; see Fig. 2. The temperature range we study, $140 < T < 280$ MeV, allows us to consider an early freeze-out of different hadrons. To be sure of the temperature independence of $J/\Psi\phi/D_s\overline{D_s}$, we next consider the possibility that the hadronization temperature T of the charm hadrons is higher than the hadronization temperature T_0 of ϕ. We study this question by exploring the sensitivity of the ratio $J/\Psi\phi/D_s\overline{D_s}$ to the two-temperature freeze-out in Fig. 3; see the bottom three lines for $T_0 = 180, 160, 140$ MeV with γ_q from the condition $S^{\rm Q} = S^{\rm H}$ in Fig. 6. If charm hadrons hadronize later, $T > T_0$ and $T - T_0 < 60$ MeV, the change in $J/\Psi\phi/D_s\overline{D_s}$ ratio is small (about 20%). If this were to be measured as an experimental result,

$$\frac{J/\Psi\phi}{D_s\overline{D_s}} \simeq 0.35\,, \qquad (12)$$

one could not but conclude that all particles involved are formed by the mechanism of statistical hadronization.

This interesting result can be understood by considering the behavior of the $\gamma_s^{\rm H}(T_0)/\gamma_s^{\rm H}(T)$ ratio, which increases rapidly with increasing $T - T_0$ (see the top three lines in Fig. 3). This ratio almost compensates for the change in ϕ yield, an effect we already encountered in the

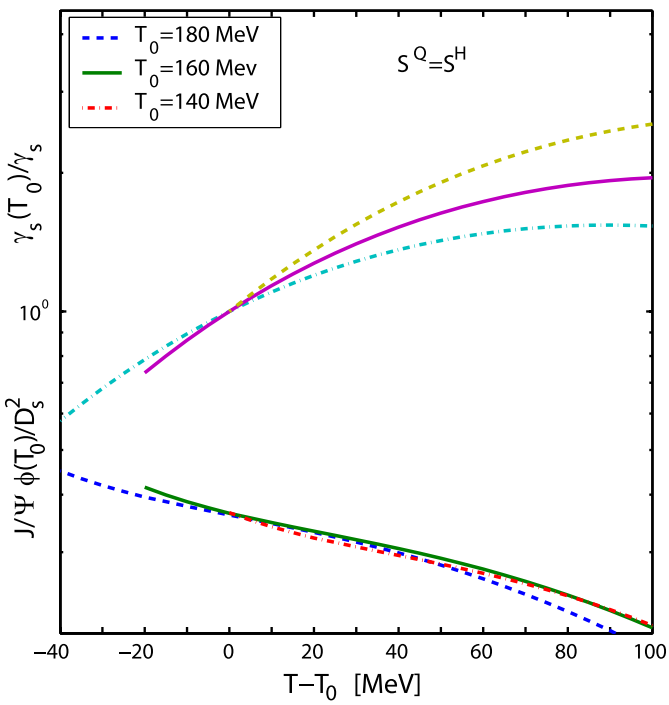

Fig. 3. The ratio $J/\Psi\,\phi(T_0)/D_sD_s$ is evaluated at two temperatures, T for heavy flavor hadrons, and T_0 for ϕ, as a function of $T - T_0$, with the three values of $T_0 = 140, 160, 180$ MeV considered with $S^{\rm H} = S^{\rm Q}$

context of the results we show below in Fig. 9. For large $T - T_0$, the ratio $J/\Psi\phi/D_s\overline{D_s}$ begins to decrease more rapidly because γ_s increases for $S^{\rm H} = S^{\rm Q}$; see Fig. 6.

4 Entropy in hadronization

4.1 Entropy in QGP fireball

The entropy content is seen in the final state multiplicity of particles produced after hadronization. More specifically, there is a relation between entropy and particles multiplicities, once we note that the entropy per particle in a gas is

$$\frac{S_{\rm B}}{N}=3.61\,,\quad \frac{S_{\rm cl}}{N}=4\,,\quad \frac{S_{\rm F}}{N}=4.2\,, \tag{13}$$

for massless Bose, classical (Boltzmann) and Fermi gases, respectively. Effectively, for QGP with the u,s,d,G degrees of freedom, $S^{\rm Q}/N^{\rm Q}\sim 4$ is applicable for a large range of masses. Thus,

$$\frac{{\rm d}S^{\rm Q}}{{\rm d}y}\approx 4\frac{{\rm d}N^{\rm Q}}{{\rm d}y}\,. \tag{14}$$

This in turn means that the final state particle multiplicity provides us with information on the primary entropy content generated in the initial state of the QGP phase.

It is today generally believed that there is an entropy conserving hydrodynamic expansion of the QGP liquid. Entropy is conserved in the fireball, and the conservation of the entropy density σ flow is expressed by

$$\frac{\partial_\mu(\sigma u^\mu)}{\partial x^\mu}=0\,, \tag{15}$$

where u^μ is a local four velocity vector. A special case of interest is the so-called Bjørken scenario [16], for which (15) can be solved exactly, assuming scaling of the physical properties as a function of rapidity as an initial condition. This implies that there is no preferred frame of reference, a situation expected in very high energy collisions. Even if highly idealized, this simple reaction picture allows for a good estimate of many physical features. Of relevance here is that the exact solution of the hydrodynamics in $(1+1)$ dimensions implies

$$\frac{{\rm d}S}{{\rm d}y}={\rm Const.} \tag{16}$$

Thus, the entropy S is not only conserved globally in the hydrodynamic expansion, but also per unit of rapidity. Though we have $(1+3)$ expansion, (16) holds as long as there is, in rapidity, a flat plateau of the particles yields. Namely, each of the domains of rapidity is equivalent, excluding the projectile–target domains. However, at RHIC and LHC energies these are causally disconnected from the central rapidity bin where we study the evolution of the heavy flavor. The entropy we observe in the final hadron state has to a large extent been produced after the heavy flavor had been produced, during the initial parton thermalization phase, but before strangeness has been produced. In order to model the production of the hadrons for different chemical freeze-out scenarios of the same reaction, we need to relate the entropy content, temperature and volume of the QGP domain. We consider the entropy content for a u,d,G chemically equilibrated QGP, and allowing for partial chemical equilibration of strangeness.

The entropy density σ can be obtained from the equation

$$\sigma\equiv\frac{S}{V}=-\frac{1}{V}\frac{{\rm d}F_{\rm Q}}{{\rm d}T}\,, \tag{17}$$

where the thermodynamic potential is

$$F_{\rm Q}(T,\lambda_q,V)=-T\ln Z({}_{\rm Q}T,\lambda_q,V)_{\rm Q}\,. \tag{18}$$

Inside QGP the partition function is a product of the partition functions of the gluons, Z_g, the light quarks, Z_q, and the strange quarks, Z_s; hence

$$\ln Z=\ln Z_g+\ln Z_q+\ln Z_s\,, \tag{19}$$

where for massless particles with $\lambda_q=1$ we have

$$\ln Z_g=\frac{g_g\pi^2}{90}VT^3\,, \tag{20}$$

$$\ln Z_q=\frac{7}{4}\frac{g_q\pi^2}{90}VT^3\,. \tag{21}$$

Here g_g is the degeneracy factor for the gluons, and g_q is the degeneracy factor for the quarks. The factor $7/4=2\cdot 7/8$ accounts for the difference in statistics and the presence of both quarks and antiquarks. The number of degrees of freedom of quarks and gluons is influenced by the strong interactions, characterized by the strong coupling constant $\alpha_{\rm s}$:

$$g_g=2_s8_c\left(1-\frac{15}{4\pi}\alpha_{\rm s}+\dots\right), \tag{22}$$

$$g_q=2_s3_c2_f\left(1-\frac{50}{21\pi}\alpha_{\rm s}+\dots\right). \tag{23}$$

The case of the strange quarks is somewhat more complicated, since we have to consider the mass, the degree of chemical equilibration, and guess an estimate for the strength of the QCD perturbative interactions. We have in the Boltzmann approximation:

$$\ln Z_s=2_{\rm p/a}\frac{g_s}{\pi^2}VT^3\,, \tag{24}$$

$$g_s=2_s3_c\gamma_s^{\rm Q}\,0.5W(m_s/T)\left(1-k\frac{\alpha_{\rm s}}{\pi}\right). \tag{25}$$

$W(m/T)$ is the function seen in (6). We allow both for strange and antistrange quarks, and we have a factor $2_{\rm p/a}$ (which for massless fermions is $2\cdot 7/8=7/4$). k at this point is a temperature dependent parameter. Even in the lowest order perturbation theory it has not been evaluated for massive quarks at finite temperature. We know that for massless quarks $k\simeq 2$. Considering an expansion in m/T, for large masses the correction reverses sign [17], which result supports the reduction in value of k for $m\simeq T$. We will use here the value $k=1$ [12].

4.2 Number of degrees of freedom in QGP

The entropy density following from (17) is

$$\sigma=\frac{4\pi^2}{90}\left(g_g+\frac{7}{4}g_q\right)T^3+\frac{4}{\pi^2}2_{\rm p/a}g_sT^3+\frac{\mathcal{A}}{T}\,. \tag{26}$$

For strange quarks in the second term in (26) we set the entropy per strange quark to 4 units. In choosing $S_s/N_s = 4$ irrespective of the effect of the interaction and of the mass value m_s/T, we are minimizing the influence of the unknown QCD interaction effect.

The last term in (26) comes from differentiation of the strong coupling constant α_s in the partition function with respect to T; see (17). Up to two loops in the β function of the renormalization group, the correction term is [18]:

$$\mathcal{A} = \left(b_0\alpha_s^2 + b_1\alpha_s^3\right)\left[\frac{2\pi}{3}T^4 + \frac{n_f 5\pi}{18}T^4\right], \qquad (27)$$

with n_f being the number of active fermions in the quark loop, $n_f \simeq 2.5$, and

$$b_0 = \frac{1}{2\pi}\left(11 - \frac{2}{3}n_f\right), b_1 = \frac{1}{4\pi^2}\left(51 - \frac{19}{3}n_f\right). \qquad (28)$$

For the strong coupling constant α_s we use

$$\alpha_s(T) \simeq \frac{\alpha_s(T_c)}{1 + C\ln(T/T_c)}, \quad C = 0.760 \pm 0.002, \qquad (29)$$

where $T_c = 0.16\,\mathrm{GeV}$. This expression arises from the renormalization group running of $\alpha_s(\mu)$, the energy scale at $\mu = 2\pi T$, and the value $\alpha_s(M_Z) = 0.118$. A much more sophisticated study of the entropy in the QGP phase is possible [19]; what we use here is an effective model that agrees with the lattice data [20, 21].

Equation (26) suggests that we introduce an effective degeneracy of the QGP based on the expression we use for the entropy:

$$g_{\mathrm{eff}}^{\mathrm{Q}}(T) = g_g(T) + \frac{7}{4}g_q(T) + 2g_s\frac{90}{\pi^4} + \frac{\mathcal{A}}{T^4}\frac{90}{4\pi^2}. \qquad (30)$$

This allows us to write

$$\sigma = \frac{4\pi^2}{90}g_{\mathrm{eff}}^{\mathrm{Q}}T^3, \qquad (31)$$

and

$$\frac{\mathrm{d}S}{\mathrm{d}y} = \frac{4\pi^2}{90}g_{\mathrm{eff}}^{\mathrm{Q}}T^3\frac{\mathrm{d}V}{\mathrm{d}y} \simeq \mathrm{Const}. \qquad (32)$$

We show the QGP degeneracy in Fig. 4, as a function of $T \in [140, 260]\,\mathrm{MeV}$, top frame for fixed $s/S = 0, 0.03, 0.04$ (from bottom to top), and in the bottom frame for the strangeness chemical equilibrium, $\gamma_s = 1$ (dashed) and for the approach to the chemical equilibrium cases (solid). When we fix the specific strangeness content s/S in the plasma comparing different temperatures, we find that in all cases $g_{\mathrm{eff}}^{\mathrm{Q}}$ increases with T. For $s/S = 0$ we have a 2-flavor system (dotted line, red), and the effective number of degrees of freedom $g_{\mathrm{eff}}^{\mathrm{Q}}$ varies between 22 and 26. The solid line with dots (green) is for $s/S = 0.03$, and the dot-dashed line (blue) gives the result for $s/S = 0.04$.

In the bottom panel of Fig. 4 we note that like for the two flavor case ($s = 0$), for the $2+1$-flavor system ($\gamma_s = 1$) $g_{\mathrm{eff}}^{\mathrm{Q}}$ increases with T (dashed line, black). $g_{\mathrm{eff}}^{\mathrm{Q}}$ varies between 30 and 35.5. The thin dashed lines indicate the range

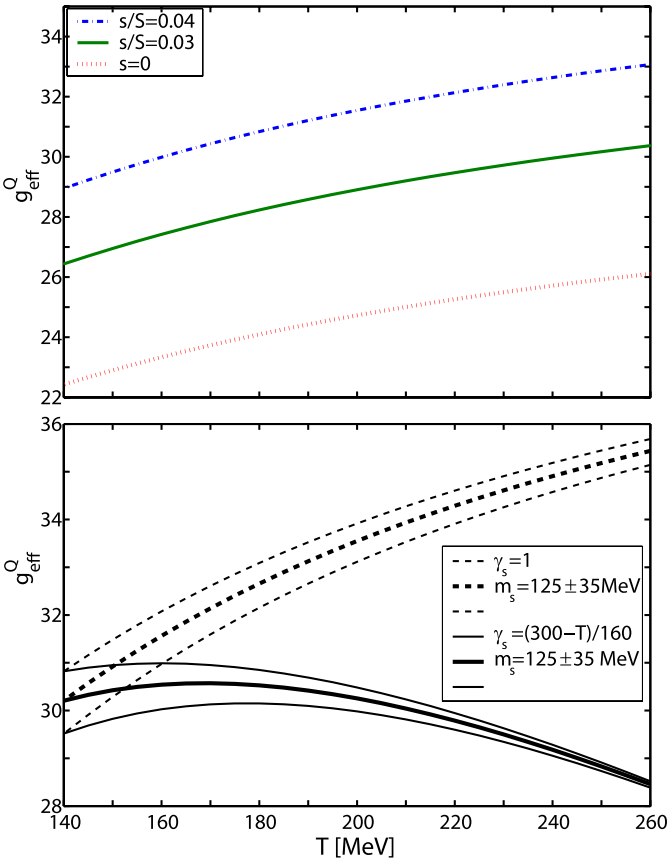

Fig. 4. The Stefan–Boltzman degrees of freedom g_{eff} based on the entropy content of QGP, as a function of temperature T. *Upper frame*: fixed s/S, the *solid line* with *dots* (*green*) is for a system with fixed strangeness per entropy $s/S = 0.03$, while the *dot-dashed* (*blue*) *line* is for $s/S = 0.04$. The *dotted* (*red*) *line* is for 2-flavor QCD $s/S = 0$ (u, d, G only); the *bottom frame* shows *dashed* (*black*) *line* $2+1$-flavor QCD with $m_s = 125 \pm 35\,\mathrm{MeV}$ (chemically equilibrated u, d, s, G system). The (*thick, thin*) *solid lines* are for QGP in which strangeness contents is increasing as a function of temperature; see text

of uncertainty due to the mass of the strange quark, which in this calculation is fixed with the upper curve corresponding to $m_s = 90\,\mathrm{MeV}$, and the lower one to $m_s = 160\,\mathrm{MeV}$. The expected decrease in value of m_s with T will thus have the effect to steepen the rise in the degrees of freedom with T.

We now explore in a QGP phase the effect of an increasing strangeness fugacity with decreasing temperature. This study is a bit different from the rest of this paper, where we consider for comparison purposes hadronization for a range of temperatures but at a *fixed* value of s/S. A variable $\gamma_s^{\mathrm{Q}}(T)$ implies a more sophisticated and thus more model dependent picture of plasma evolution. However, this offers us important insight in $g_{\mathrm{eff}}^{\mathrm{Q}}$.

We consider the function

$$\gamma_s^{\mathrm{Q}} = \frac{300 - T[\mathrm{MeV}]}{160}. \qquad (33)$$

This is consistent with the kinetic computation of the strangeness production [12]. At $T = 140\,\mathrm{MeV}$ we have chemical equilibrium in the QGP phase, while at the temperature $T = 260\,\mathrm{MeV}$ we have $\gamma_s = 0.25$. The result for $g^{\mathrm{Q}}_{\mathrm{eff}}$ is shown as a thick (black) line in Fig. 4, with the range showing the strange quark mass range $m_s = 125 \pm 35\,\mathrm{MeV}$. We see that in a wide range of temperatures we have $29.5 < g^{\mathrm{Q}}_{\mathrm{eff}} < 30.5$.

The lesson is that with the growth of γ_s^{Q} with decreasing T the entropy of the QGP is well described by the constant value $g^{\mathrm{Q}}_{\mathrm{eff}} = 30 \pm 0.5$. Since the entropy is (nearly) conserved and $g^{\mathrm{Q}}_{\mathrm{eff}}$ is (nearly) constant, (32) implies that we can scale the system properties using the constraint $T^3 \mathrm{d}V/\mathrm{d}y = \mathrm{Const}$. We stress again that these results arise in a realistic QGP with $2+\gamma_s^{\mathrm{Q}}$ flavors, but they are model dependent and of course rely on the lattice motivated description of the behavior of the QGP properties. On the other hand, it is not surprising that the rise of the strangeness chemical saturation with decreasing temperature compensates the 'freezing' of the q, G degrees of freedom with decreasing temperature.

4.3 Entropy content and chemical (non-) equilibrium

We use as a reference a QGP state with $\mathrm{d}V/\mathrm{d}y = 800\,\mathrm{fm}^3$ at $T = 200\,\mathrm{MeV}$; see Table 2. We find from (14) the Q and H phase particle multiplicity. The hadron multiplicity stated is what results after secondary resonance decays. The total hadron multiplicity after hadronization and resonance decays was calculated using the on-line SHARE 2.1 package [22, 23]. If a greater (smaller) yield of final state hadrons is observed at LHC, the value of $\mathrm{d}V/\mathrm{d}y$ need to be revised up (down). In general, expansion before hadronization will not alter $\mathrm{d}S/\mathrm{d}y$. We can expect that as T decreases, $V^{1/3}$ increases. Stretching the validity of (32) to low temperature, $T = 140\,\mathrm{MeV}$, we see the result in the second line of Table 2.

For QGP, in general the entropy content is higher than in a comparable volume of chemically equilibrated hadron matter, because of the liberation of color degrees of freedom in the color-deconfined phase. The total entropy has to be conserved during the transition between the QGP and HG phases, and thus after hadronization, the excess of entropy is observed in excess particle multiplicity, which can be interpreted as a signature of deconfinement [24, 25]. The dynamics of the transformation of QGP into HG determines how this additional entropy manifests itself.

The comparison of entropy in both phases is temperature dependent, but in the domain of interest, i.e. $140 < T < 180\,\mathrm{MeV}$, the entropy density follows

$$\sigma^{\mathrm{Q}} \gtrsim 3\sigma^{\mathrm{H}}\,. \tag{34}$$

Since the total entropy S is conserved or slightly increases, in the hadronization process some key parameter must grow in the hadronization process. There are two options:

a) either the volume changes:

$$3V^{\mathrm{H}} \gtrsim V^{\mathrm{Q}}; \tag{35}$$

b) the phase occupancies change, and since $n_i \propto \gamma_i^{2,3}, i = q, s$ in the hadron phase

$$\gamma_q^{\mathrm{H}} \simeq \sqrt{3}\,, \quad \gamma_s^{\mathrm{H}}/\gamma_q^{\mathrm{H}} \gtrsim 1\,. \tag{36}$$

In a slow transition, on the hadronic time scale, such as is the case in the early Universe, we can expect that case a) prevails. In high energy heavy-ion collisions, there is no evidence in the experimental results for the long coexistence of hadron and quark phases which is required for volume growth. Consequently, we have $V^{\mathrm{H}} \sim V^{\mathrm{Q}}$ and a large value of γ_q^{H} is required to conserve entropy. The value of γ_q^{H} is restricted by

$$\gamma_q^{\mathrm{cr}} \cong \exp\left(m_{\pi^0}/2T\right). \tag{37}$$

This value, γ_q^{cr}, is near to maximum allowed value, which arises under the conditions of Bose–Einstein condensation of pions. We will discuss quantitative results for γ_q^{H} (and γ_s^{H}) below, in Sect. 5.4.

Table 2. Reference values of volume, temperature, entropy, particle multiplicity

$\mathrm{d}V/\mathrm{d}y\ [\mathrm{fm}^3]$	T [MeV]	$\mathrm{d}S^{\mathrm{Q}}/\mathrm{d}y$	$\mathrm{d}N^{\mathrm{Q}}/\mathrm{d}y$	$\mathrm{d}N^{\mathrm{H}}/\mathrm{d}y$
800	200	10 970	2700	5000
2300	140	10 890	2700	4500

5 Strangeness in hadronization

5.1 Abundance in QGP and HG

The efficiency of the strangeness production depends on the energy and collision centrality of the heavy-ion collisions. The increase, with the value of the centrality (participant number), of the specific yield of the strangeness per baryon indicates the presence of a strangeness production mechanism acting beyond the first collision dynamics. The thermal gluon fusion to strangeness can explain this behavior [8], and a model of the flow dynamics at RHIC and LHC suggests that the QGP approaches chemical equilibrium but also can exceed it at the time of hadronization [12].

The strangeness yield in a chemically equilibrated QGP is usually described as an ideal Boltzmann gas. However, a significant correction is expected due to perturbative QCD effects. We implement this correction based on the comments below (25). We here use the expression

$$\frac{\mathrm{d}N_s^{\mathrm{Q}}}{\mathrm{d}y} = \gamma_s^{\mathrm{Q}} \left(1 - \frac{\alpha_{\mathrm{s}}}{\pi}\right) n_s^{\mathrm{eq}} \frac{\mathrm{d}V}{\mathrm{d}y}\,. \tag{38}$$

with the Boltzmann limit density (5) and the mass $m_s = 125\,\mathrm{MeV}$, and with $g_s = 6$ and $\lambda_s = 1$. The QCD correction corresponds to the discussion of the entropy in Sect. 4.1.

We obtain the strange quark phase space occupancy $\gamma_s^{\rm H}$ as a function of temperature from the condition of the equality of the numbers of strange quark and antiquark pairs in QGP and HG. Specifically, in the case of sudden QGP hadronization, quarks recombine and we expect that the strangeness content does not significantly change. For heavier flavors across the phase boundary this condition (9) is very well satisfied; for strangeness the fragmentation effect adds somewhat to the yield,

$$\frac{{\rm d}N_s^{\rm H}}{{\rm d}y} \gtrsim \frac{{\rm d}N_s^{\rm Q}}{{\rm d}y}\,. \tag{39}$$

Using the equality of the yields we slightly underestimate the value of the strangeness occupancy that results. We recall that we also conserve the entropy (10), which, like strangeness, can in principle grow in the hadronization,

$$\left.\frac{s}{S}\right|_{\rm H} \gtrsim \left.\frac{s}{S}\right|_{\rm Q}\,, \tag{40}$$

using (10), and we underestimate the value of $\gamma_q^{\rm H\,2}$.

Counting all strange particles, the number of pairs is

$$\frac{{\rm d}N_s^{\rm H}}{{\rm d}y} = \frac{{\rm d}V}{{\rm d}y}\left[\gamma_s^{\rm H}\left(\gamma_q^{\rm H} n_K^{\rm eq} + \gamma_q^{\rm H\,2} n_Y^{\rm eq}\right) + \gamma_s^{\rm H\,2}\left(2\gamma_q^{\rm H} n_\Xi^{\rm eq} + n_\phi^{\rm eq} + P_s n_\eta^{\rm eq}\right) + 3\gamma_s^{\rm H\,3} n_\Omega^{\rm eq}\right], \tag{41}$$

where the $n_i^{\rm eq}$ are the densities of the strange hadrons (mesons and baryons) calculated using (4) in chemical equilibrium. P_s is the strangeness content of the η. We count hadrons is by following the strangeness content, for example, $n_K^{\rm eq} = n_{K^+}^{\rm eq} + n_{K^0}^{\rm eq} = n_{K^-}^{\rm eq} + n_{\bar K^0}^{\rm eq}$. We impose in our calculations $\bar s = s$. The pattern of this calculation follows an established approach, by using SHARE 2.1 [22, 23] in a detailed evaluation.

5.2 Strangeness per entropy s/S

Considering both strangeness and entropy to be conserved in the hadronization process, a convenient variable to consider as fixed in the hadronization process is the ratio of these conserved quantities, s/S. In chemical equilibrium we expect that in general such a ratio must be different for different phases of matter from which particles are produced [12, 26, 27].

We compare for QGP and HG the specific strangeness per entropy content in Fig. 5. We show as a function of temperature T the s/S ratios for the chemically equilibrated QGP and HG phases. For the QGP the entropy S in QGP is calculated as described in Sect. 4, and we use $k = 1$ in (38). The shaded area shows the range of masses of the strange quarks considered; results are for $m_s = 90$ MeV (upper (blue) dash-dotted line) and $m_s = 160$ MeV ((green) solid line) forming the boundaries. The central QGP value is at about $s/S = 0.032$.

The short-dashed (light blue) line shows the hadron phase s/S value found using SHARE 2.1. For HG close

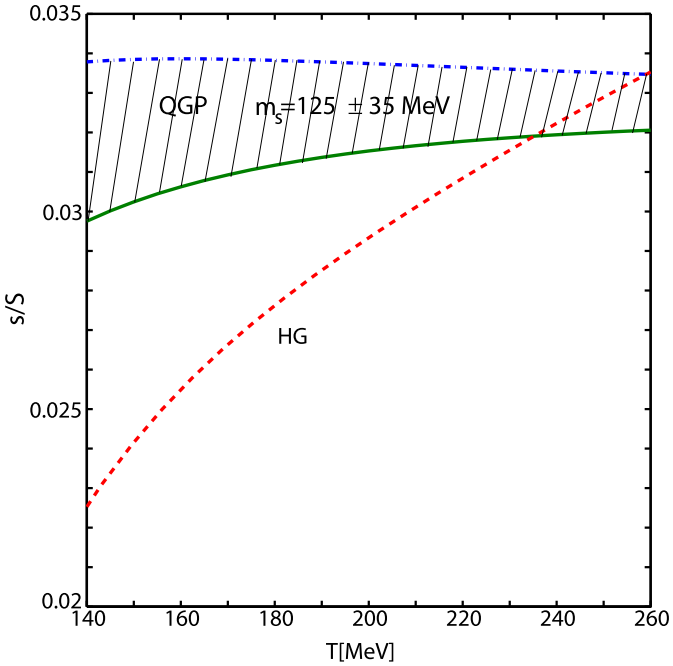

Fig. 5. Strangeness to entropy ratio s/S as a function of temperature T, for the QGP (*green, solid line* for $m_s = 160$ MeV, *blue dash-dot line* for $m_s = 90$ MeV) with $k = 1$, see (38); and for the HG (*light blue, dashed line*) phases for $\gamma_q = \gamma_s = \lambda_q = \lambda_s = 1$ in both phases

to the usual range of the hadronization temperature, $T \simeq 160$ MeV, we find $s/S \simeq 0.025$. In general, the formation of QGP implies an increase by 30% in s/S. Both the HG and the QGP phase has a similar specific strangeness content at $T = 240$–260 MeV; however, it is not believed that a HG at such a high temperature would be a stable form of matter. This HG to QGP dissociation or QGP hadronization depends on the degree of strangeness equilibration in the plasma [32] and on other dynamical factors.

In the QGP the value of s/S for the range of a realistic hadronization temperature, $140 < T < 180$ MeV, is in general larger than in HG. This implies that, generally, the abundance of strange hadrons produced in hadronization oversaturates the strange hadron phase space, if the QGP state had reached (near) chemical equilibrium. Moreover, since we are considering the ratio s/S and find in QGP a value greater than in HG, for chemical equilibrium in QGP, the hadronization process will lead to $\gamma_s^{\rm H}/\gamma_q^{\rm H} > 1$.

One may wonder if we have not overlooked some dynamical or microscopic effect that could adjust the value of s/S implied by QGP to the value expected in HG. First we note that fast growth of the volume V cannot change s/S. Moreover, any additional strangeness production in hadronization would enhance the overabundance recorded in the resulting HG. Only a highly significant entropy production at fixed strangeness yield in the hadronization process could bring the QGP s/S ratio down, masking strangeness oversaturation. No mechanism for such an entropy production in hadronization is known, and, moreover, this would further entail an unexpected and high hadron multiplicity excess.

One could of course argue that the perturbative QCD properties in the QGP are meaningless; the entropy in QGP is much higher at a given temperature. However, the properties of QGP have been checked against the lattice results, and the use of lowest order expressions is justified in these terms [20, 21]. Moreover, the value of s/S is established way before hadronization.

5.3 Wróblewski ratio W_s

At this point it is appropriate to look at another observable proposed to study the strangeness yield, the Wróblewski ratio [28]:

$$W_s \equiv \frac{2\langle \bar{s}s\rangle}{\langle \bar{u}u\rangle + \langle \bar{d}d\rangle}\,. \tag{42}$$

W_s compares the number of newly produced strange quarks to the number of light quarks produced. In an equilibrated deconfined phase W_s compares the number of active strange quark degrees of freedom to the number of light quark degrees of freedom.

The ratio s/S compares the strange quark degrees of freedom to all degrees of freedom available in QGP. Therefore as a function of T the ratios s/S and W_s can behave differently: considering the limit $T \to T_c$, a constant s/S indicates that the reduction of s degrees of freedom goes hand in hand with the 'freezing' of gluon degrees of freedom, which precedes the 'freezing' of light quarks. This also implies that for $T \to T_c$ in general W_s diminishes. The magnitude of m_s, the strange quark mass, decisively enters the limit $T \to T_c$.

For $T \gg T_c$ the ratio W_s can be evaluated comparing the rates of production of light and strange quarks, using the fluctuation–dissipation theorem [29], which allows us to relate the rate of quark production to quark susceptibilities χ_i (see (11) and (12) in [29]):

$$W_s \simeq R_\chi = \frac{2\chi_s}{\chi_u + \chi_d}\,. \tag{43}$$

The evaluation of R_χ as a function of temperature in lattice QCD has been achieved [30, 31]. For $T \simeq 2.5T_c$ the result obtained, $W_s \to R_\chi \simeq 0.8$, is in agreement with the expectation for equilibrium QGP with nearly free quarks, with strangeness mass having a small but noticeable significance. With decreasing T, the ratio $R_\chi \to 0.3$ for $m_s = T_c$. However, this value of m_s is too large; the physical value should be nearly half as large, which would result in a greater R_χ. Moreover, for $T \to T_c$ the relationship of W_s to R_χ, (43) is in question, in that the greatly reduced rate of production of strangeness may not be satisfying the conditions required in [29].

Comparing the observables s/S and W_s we note that the experimental measurement requires in both cases a detailed analysis of all particles produced. At lower reaction energies there is an additional complication in the evaluation of W_s due to the need to subtract the effect of the quarks brought about in the reaction region. Turning to the theoretical computation of s/S and W_s we note that the thermal lattice QCD evaluation of s/S is possible without any approximation, even if the actual computation of entropy near the phase boundary is a challenging task. On the other hand, the lattice computation of W_s relies on the production rate of strangeness being sufficiently fast, which cannot be expected near the phase boundary. Moreover, the variable s/S probes all QGP degrees of freedom, while W_s probes only the quark degrees of freedom. We thus conclude that s/S is both more accessible theoretically and experimentally, and perhaps an observable more related to QGP, as compared to W_s, since it comprises the gluon degrees of freedom.

5.4 Strangeness chemical non-equilibrium

In order to have continuity of strangeness, (39), and entropy, (40), in fast hadronization, the hadron phase should obey $\gamma_s^{\rm H} \neq 1$ and $\gamma_q^{\rm H} \neq 1$. We have to solve for $\gamma_s^{\rm H}$ and $\gamma_q^{\rm H}$ simultaneously in (39) and (40).

In Fig. 6 we show as a function of T the strange phase space occupancy $\gamma_s^{\rm H}$, obtained for several values of the ratio s/S (from top to bottom 0.045, 0.04, 0.035, 0.03, 0.025) evaluated for $S^{\rm Q} = S^{\rm H}$. The solid line shows $\gamma_q^{\rm H}$ for $s^{\rm Q} = s^{\rm H}$ and $S^{\rm Q} = S^{\rm H}$. The maximum allowed value (37) is shown by dashes (red).

In Fig. 7 we show the results for $\gamma_s^{\rm H}/\gamma_q^{\rm H}$ (where $\gamma_q^{\rm H} = 1$ we show $\gamma_s^{\rm H}$). We consider the three cases of $\gamma_q = 1$, $\gamma_q^{\rm H} =$

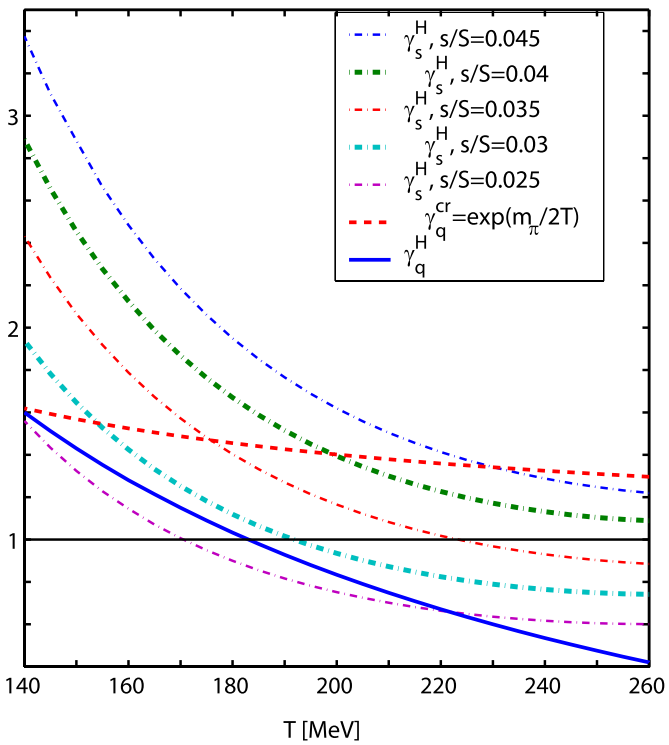

Fig. 6. Phase space occupancy as a function of T: $\gamma_q^{\rm H}$ (*blue, solid line*), $\gamma_s^{\rm H}$ (*dash-dotted lines*, from top to bottom) for $s/S = 0.045$, for $s/S = 0.04$ (*thick line*), $s/S = 0.035$, $s/S = 0.03$ (*thick line*), $s/S = 0.025$; $\gamma_q^{\rm cr}$ (*red, dashed line*)

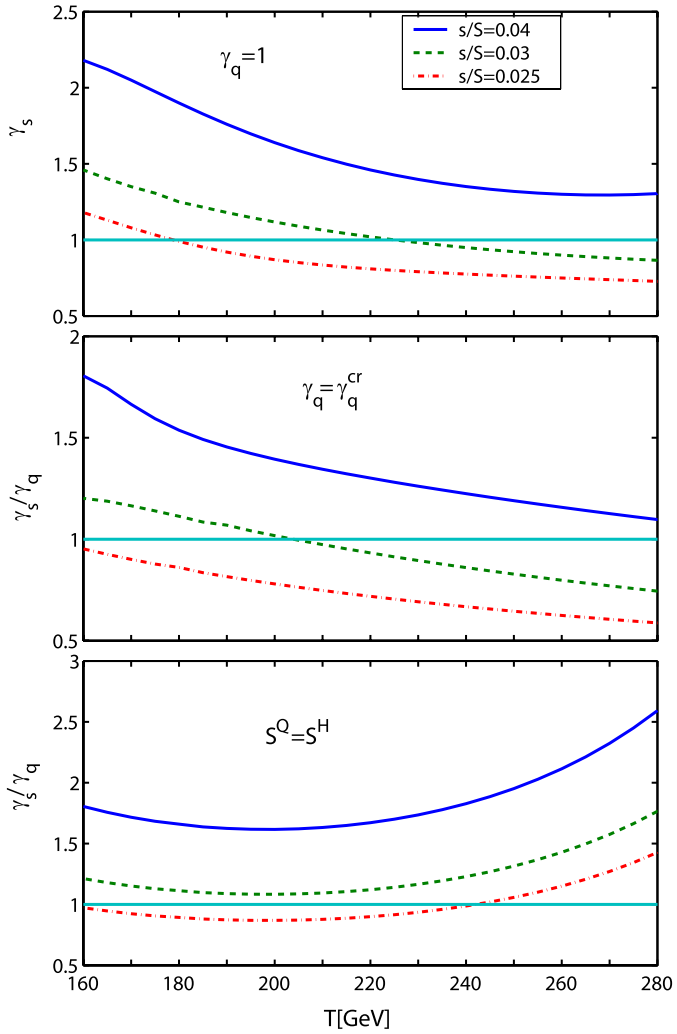

Fig. 7. $\gamma_s^{\rm H}/\gamma_q^{\rm H}$ ($=\gamma_s^{\rm H}$ at $\gamma_q^{\rm H}=1$) as a function of the hadronization temperature T. Top frame: $\gamma_q^{\rm H}=1$, middle frame: $\gamma_q^{\rm H}=\gamma_q^{\rm cr}$, and bottom frame: $S^H=S^{\rm Q}$. *Lines*, from top to bottom: $s/S=0.04$ (*blue, solid line*), $s/S=0.03$ (*green, dashed line*), $s/S=0.025$ (*red, dash-dot line*)

$\gamma_q^{\rm cr}$ and entropy conservation, $S^{\rm H}=S^{\rm Q}$, for $s/S=0.045$, $s/S=0.04$, $s/S=0.035$, $s/S=0.03$, $s/S=0.025$ (dash-dot lines) (lines from top to bottom). We see that except for the case that strangeness were to remain well below chemical equilibrium in QGP ($s/S\simeq 0.03$), the abundance of the heavy flavor hadrons that we will turn to in a moment will be marked by an overabundance of strangeness, since practically in all realistic conditions we find $\gamma_s^{\rm H}>\gamma_q^{\rm H}$.

In Fig. 8 we show the ratio s/S as a function of $\gamma_s^{\rm H}/\gamma_q^{\rm H}$. The solid line is for $T=200$ MeV, $\gamma_q^{\rm H}=0.83$ and $S^{\rm Q}=S^{\rm H}$, the dashed line for $T=170$ MeV, $\gamma_q^{\rm H}=1.15$ and $S^{\rm Q}=S^{\rm H}$ and the dash-dotted line for $T=140$ MeV, $\gamma_q^{\rm H}=1.6$ MeV and $S^{\rm Q}=S^{\rm H}$. We also consider the case $\gamma_q=1$ for $T=170$ MeV (dot marked (purple) solid line). In this case, the strangeness content γ_s/γ_q is higher than for $S^{\rm H}=S^{\rm Q}$ with the same T and s/S. In the limit $\gamma_q^{\rm H}=\gamma_q^{\rm cr}$, (37), ($T=200$ MeV, solid, thin line; $T=170$ MeV, dashed line)

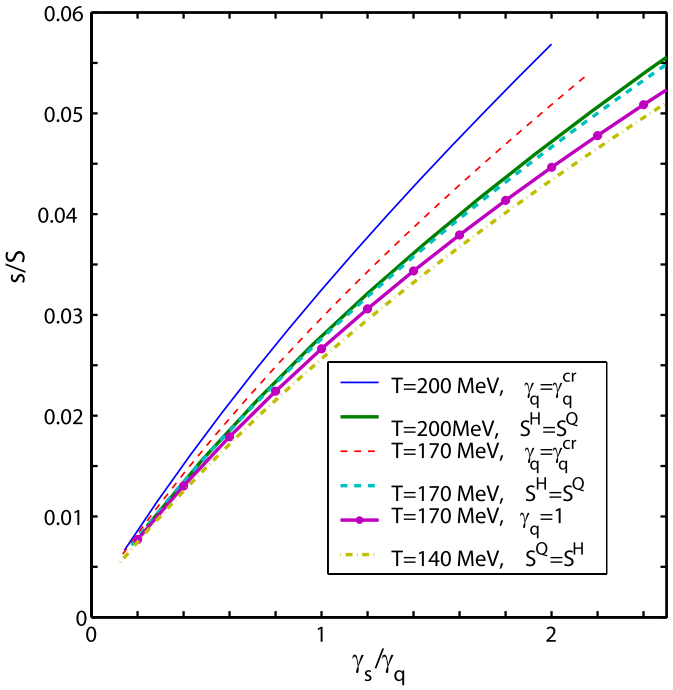

Fig. 8. Strangeness to entropy ratio, s/S, as a function of γ_s/γ_q for $T=200$ MeV, $\gamma_q=0.083$, $S^{\rm H}=S^{\rm Q}$(*solid line*), $T=170$ MeV, $\gamma_q=1.15$, $S^{\rm H}=S^{\rm Q}$ (*dashed line*), $T=140$ MeV, $\gamma_q=1.6$, $S^{\rm H}=S^{\rm Q}$ (*dash-dotted line*); $\gamma_q=1$ (*dot marked solid*); $\gamma_q=\gamma_q^{\rm cr}$: $T=200$ MeV (*thin solid line*), $T=170$ MeV (*thin dashed line*)

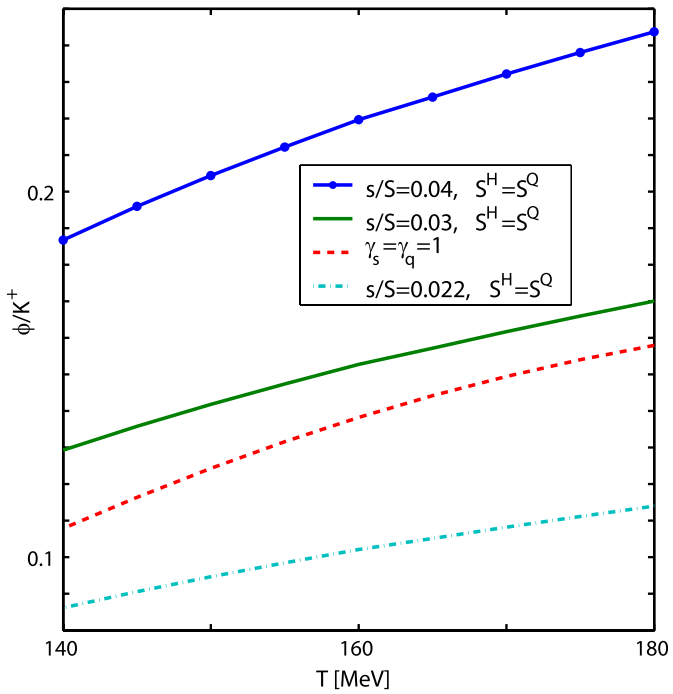

Fig. 9. The ratio $\phi/{\rm K}^+$ as a function of T. The *dashed line* (*red*) is for chemical equilibrium. The *solid line* with *dots* (*green*) is for $s/S=0.03$, the *solid line* (*blue*) for $s/S=0.04$, the *dash-dot line* (*per*) is for $s/S=0.022$

Table 3. Specific and absolute strangeness yield for different reaction volumes at $T = 200$ MeV

s/S	$\mathrm{d}s/\mathrm{d}y$	$\mathrm{d}V/\mathrm{d}y$ [fm^{-3}]	T [MeV]
0.045	550	1000	200
0.04	360	800	200
0.035	250	700	200
0.03	165	600	200
0.025	106	500	200
0.022	83	500	200

the strangeness content $\gamma_s^{\mathrm{H}}/\gamma_q^{\mathrm{H}}$ is minimal for given T and s/S.

These results suggest that it is possible to measure the value of s/S irrespective of what the hadronization temperature may be, as long as the main yield dependence is on the ratio $\gamma_s^{\mathrm{H}}/\gamma_q^{\mathrm{H}}$. Indeed, we find that the ratio ϕ/K^+,

$$\frac{\phi}{K^+} = \frac{\gamma_s^{\mathrm{H}}}{\gamma_q^{\mathrm{H}}} \frac{n_\phi^{\mathrm{eq}}}{n_{K^+}^{\mathrm{eq}}}\,, \tag{44}$$

is less sensitive to the hadronization temperature compared to its strong dependence on the value of s/S. In Fig. 9 we show the total hadron phase space ratio ϕ/K^+ as a function of T for several s/S ratios, and for $\gamma_{s,q}^{\mathrm{H}} = 1$ (chemical equilibrium, dashed (red) line). The K^+ yield contains the contribution from the decay of ϕ into kaons, which is a noticeable correction.

We record in Table 3 for given s/S and volume $\mathrm{d}V/\mathrm{d}y$ the corresponding total yields of the strangeness, which may be a useful guide in consideration of the consistency of experimental results with what we find exploring the heavy flavor hadron abundance.

6 Yields of heavy flavored hadrons

6.1 Phase space occupancy γ_c^{H} and γ_b^{H}

The first step in order to determine the yields of heavy flavor hadronic particles is the determination of the phase space occupancy γ_c^{H} and γ_b^{H}. γ_c^{H} is obtained from the equality of the numbers of these quarks (i.e. of quark and antiquark pairs) in QGP and HG. The yield constraint is

$$\frac{\mathrm{d}N_c}{\mathrm{d}y} = \frac{\mathrm{d}V}{\mathrm{d}y}\left[\gamma_c^{\mathrm{H}} n_{\mathrm{op}}^c + \gamma_c^{\mathrm{H}\,2}(n_{\mathrm{hid}}^{c\,\mathrm{eq}} + 2\gamma_q^{\mathrm{H}} n_{ccq}^{\mathrm{eq}} + 2\gamma_s^{\mathrm{H}} n_{ccs}^{\mathrm{eq}})\right]; \tag{45}$$

where the open 'op' charm yield is

$$n_{\mathrm{op}}^c = \gamma_q^{\mathrm{H}} n_D^{\mathrm{eq}} + \gamma_s^{\mathrm{H}} n_{D_s}^{\mathrm{eq}} + \gamma_q^{\mathrm{H}\,2} n_{qqc}^{\mathrm{eq}} + \gamma_s^{\mathrm{H}}\gamma_q^{\mathrm{H}} n_{sqc}^{\mathrm{eq}} + \gamma_s^{\mathrm{H}\,2}\, n_{ssc}^{\mathrm{eq}}\,. \tag{46}$$

Here n_D^{eq} and $n_{D_s}^{\mathrm{eq}}$ are the densities of the D and D_s mesons, respectively, in chemical equilibrium, and n_{qqc}^{eq} is the equilibrium density of the baryons with one charm and two light quarks; n_{ssc}^{eq} is the density of the baryons with one charm (or later on one bottom quark) and two strange quarks (Ω_c^0, Ω_b^0) in chemical equilibrium and finally $n_{\mathrm{hid}}^{\mathrm{eq}}$ is the equilibrium particle density with both a charm (or bottom) and an anticharm (or antibottom) quark ($C = 0$, $B = 0, S = 0$). The equilibrium densities can be calculated using (4). γ_c^{H} can now be obtained from (45).

Similar calculations can be done for γ_b^{H}. The only difference is that we need to add the number of B_c mesons to the right hand side of (45),

$$\frac{\mathrm{d}N_{B_c}}{\mathrm{d}y} = \gamma_b^{\mathrm{H}}\gamma_c^{\mathrm{H}} n_{B_c}^{\mathrm{eq}} \frac{\mathrm{d}V}{\mathrm{d}y}\,. \tag{47}$$

$n_{B_c}^{\mathrm{eq}}$ is the density in chemical equilibrium of B_c. In the calculation of γ_c^{H} the contribution of the term with n_{B_c} is very small, and we did not consider it above.

The value of γ_c is in essence controlled by the open single charm mesons and baryons. For this reason we do not consider the effect of exact charm conservation. The relatively small effects due to the canonical phase space of charm are leading to a slight up-renormalization of the value of γ_c, so that the primary $\mathrm{d}N_c/\mathrm{d}y$ yield is preserved. This effect enters into the yields of multi-charm and hidden charm hadrons, where the compensation is not exact, and there remains a slight change in these yields. However, the error made considering the high yield of charm is not important. On the other hand, for multi-bottom and hidden bottom hadrons the canonic effect can be large, depending on the actual bottom yield, and thus we will not discuss in this paper the yields of these hadrons, pending an extension of the methods here developed to include the canonical phase space effect.

We consider in Fig. 10 the temperature dependence of both γ_b^{H} (top) and γ_c^{H} (bottom) for the heavy flavor yield given in (1) and (2)). In the non-equilibrium case (solid lines) the space occupancy γ_s^{H} is obtained from (41), and γ_q^{H} is chosen to keep $S^{\mathrm{H}} = S^{\mathrm{Q}}$. The $\gamma_{c(b)}^{\mathrm{H}}$ depend on γ_s and γ_q: the value of N_s in (41) is chosen to have $s/S = 0.04$ after hadronization, the corresponding γ_q^{H} and γ_s^{H} are shown in Figs. 6 and 7. Since the applicable γ_q^{H} may depend on the hadronization dynamics and/or details of the equation of state of QGP, we show the charm quark phase space occupancies also for the maximal possible value of $\gamma_q^{\mathrm{H}} \to \gamma_q^{\mathrm{cr}}$), also considered at $s/S = 0.04$ for all hadronization temperatures. We can compare our results with the chemical equilibrium (dashed lines) setting $\gamma_s^{\mathrm{H}} = \gamma_q^{\mathrm{H}} = 1$ in (45). Under hadronization conditions, with temperatures $T = 160 \pm 20$ MeV we see in Fig. 10 a significant difference (considering the fast changing logarithmic scale) between the chemical equilibrium and non-equilibrium ($s/S = 0.04$) results.

In Fig. 11 we show the ratio $\gamma_{c(b)}^{\mathrm{H}}/\gamma_{c(b)\,\mathrm{eq}}^{\mathrm{H}}$ as a function of the hadronization temperature T. This helps us to understand when the presence of chemical non-equilibrium is most noticeable. This is especially the case should heavy flavor hadronization occur at the same temperature, $T = 140$–170 MeV, as is obtained for non-heavy hadrons, and/or when the entropy content of the light hadrons is maximized with $\gamma_q^{\mathrm{H}} \to \gamma_q^{\mathrm{cr}}$. When no additional entropy is

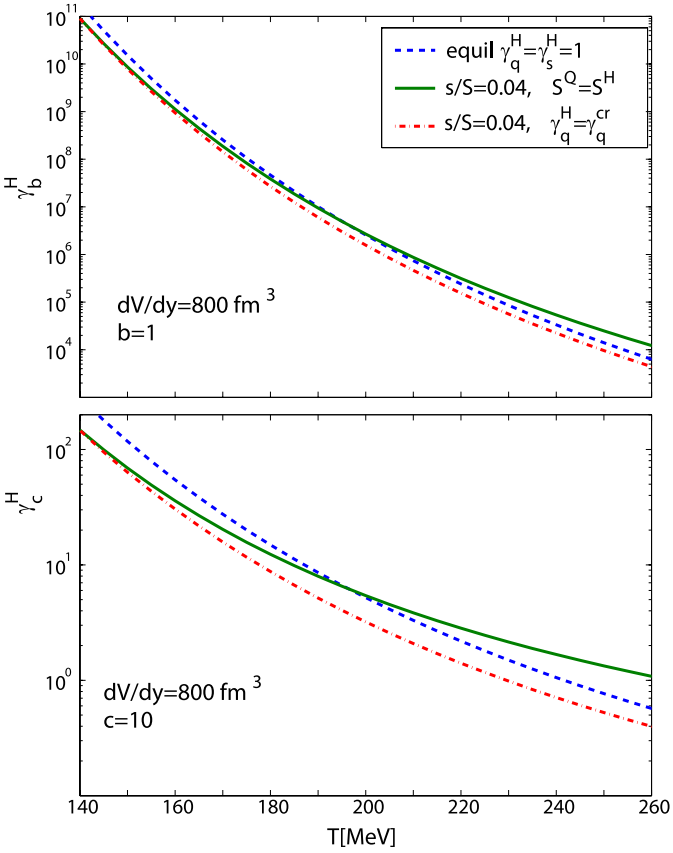

Fig. 10. $\gamma_b^{\rm H}$ ($b=1$) (*upper panel*), and $\gamma_c^{\rm H}$ ($c=10$) (*lower panel*), as functions of the temperature of the hadronization T. The *solid lines* are non-equilibrium for $s/S=0.04$ with $S^{\rm Q}=S^{\rm H}$, the *dashed lines* are for the equilibrium case $\gamma_s=\gamma_q=1$ and the *dot-dash lines* are for $s/S=0.04$ with the maximal value of γ_q ($\gamma_q=\gamma_q^{\rm cr}$) (${\rm d}V/{\rm d}y=800\,{\rm fm}^3$)

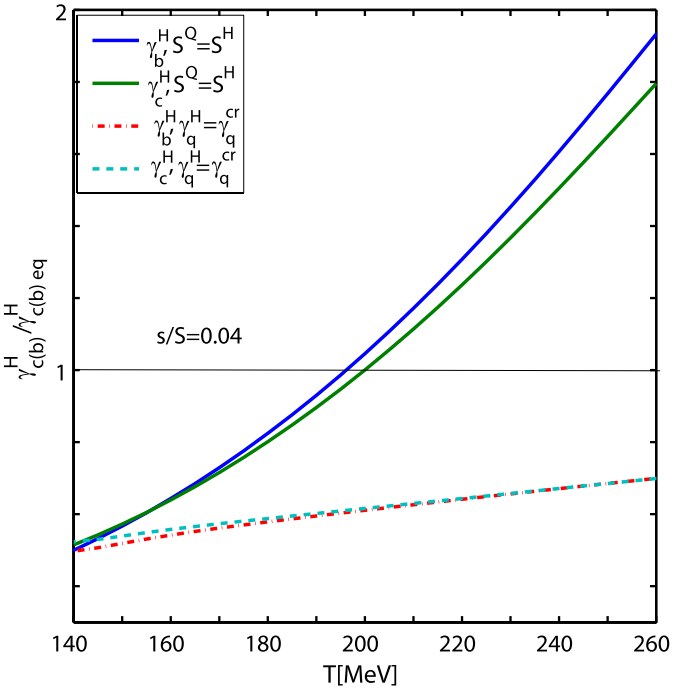

Fig. 11. $\gamma_b^{\rm H}/\gamma_{b\,{\rm eq}}^{\rm H}$ and $\gamma_c^{\rm H}/\gamma_{c\,{\rm eq}}^{\rm H}$, as functions of the temperature of the heavy flavor hadronization T. The *solid* with *dot marks line* is for $\gamma_b^{\rm H}/\gamma_{b\,{\rm eq}}^{\rm H}$ with $s/S=0.04$, the *solid line* is for $\gamma_c^{\rm H}$ with $s/S=0.04$, the *dot-dash* and *dashed lines* are for $s/S=0.04$ with the maximal value of $\gamma_q\to\gamma_q^{\rm cr}$ for $\gamma_b^{\rm H}/\gamma_{b\,{\rm eq}}^{\rm H}$ and for $\gamma_c^{\rm H}/\gamma_{c\,{\rm eq}}^{\rm H}$, respectively

formed in the hadronization, that is, $S^{\rm H}=S^{\rm Q}$, $\gamma_{c(b)}^{\rm H}/\gamma_{c(b)\,{\rm eq}}^{\rm H}$ exceeds unity for $T>200\,{\rm MeV}$, at which point the heavy flavor hadron yields exceed the chemical equilibrium expectations. In general, we find that heavy hadron yields, if produced at normal hadronization temperatures, would be effectively suppressed, compared to statistical equilibrium results, by the high strangeness yield. This happens since the phase space is bigger at $\gamma_{s,q}^{\rm H}>1$, and thus a smaller $\gamma_{c,b}^{\rm H}$ is required to reach a given heavy flavor yield.

$\gamma_b^{\rm H}$ and $\gamma_c^{\rm H}$ are nearly proportional to ${\rm d}N_{b,c}/{\rm d}y$, respectively. The deviation from the proportionality is due to the abundance of multi-heavy hadrons, and it is small. To estimate this effect more quantitatively we first evaluate

$$\gamma_{c0}^{\rm H}=\frac{{\rm d}N_c}{{\rm d}y}\Big/\left(\frac{{\rm d}V}{{\rm d}y}n_{\rm open}^c\right), \qquad (48)$$

i.e. the value expected in the absence of multi-heavy hadrons. Next we compare with the result when we take into account the last three terms in (45). The influence of these terms not only depend on ${\rm d}N_c/{\rm d}y$ but also on ${\rm d}N_c/{\rm d}y/{\rm d}V/{\rm d}y$. For fixed ${\rm d}V/{\rm d}y=800\,{\rm fm}^{-3}$ in the range of ${\rm d}N_c/{\rm d}y=(5,30)$, we find that $\gamma_c^{\rm H}/N_c$ (and therefore the yields of the open charm hadrons) changes at a temperature of $T=140\,{\rm MeV}$ by $\sim 6\%$ for $s/S=0.04$. For the chemical equilibrium case, $\gamma_s=\gamma_q=1$, $\gamma_c^{\rm H}/N_c$ changes up to 15% at the same conditions. For the particles with hidden charm or two charm quarks, the yields are proportional to γ_i^2, and therefore changes in their yields will be about twice larger. For RHIC $N_c<3$ and ${\rm d}V/{\rm d}y=600\,{\rm fm}^{-3}$; the dependence of the yields on N_c is much smaller.

The multiplicity ${\rm d}N_c/{\rm d}y$ can also influence $\gamma_b^{\rm H}$, since, as we noted, it also includes a term proportional to $\gamma_c^{\rm H}n_{B_c}^{\rm eq}$. In the range of $N_c=(5,30)$, γ_b/N_b changes at a temperature of $T=0.14\,{\rm MeV}$ by $\sim 0.5\%$ for $s/S=0.04$. Since the mass of the b quark is much larger than that of the c quark, the effect due to multi-bottom states is negligible.

6.2 D, D_s, B, B_s meson yields

In the next sections we will mostly consider the particle yields after hadronization and we will omit the superscript H in the γ. Considering (4), we first obtain γ_c as a function of the ratio γ_s/γ_q and T. Substituting this γ_c and the appropriate equilibrium hadron densities into (4), we obtain the yields of $D(B)$ and $D_s(B_s)$, as functions of the ratio γ_s/γ_q, at fixed temperature, which are shown on Fig. 12. In the upper panel we show the fractional yields of the charm D/N_c and D_s/N_c mesons, and in the lower panel B/N_b and B_s/N_b for $T=200\,{\rm MeV}$ (solid line), $T=170\,{\rm MeV}$ (dashed

line), $T = 140\,\mathrm{MeV}$ (dash-dot line). The fractional yield means that these yields are normalized by the total number of charm quarks N_c and bottom quarks N_b, and thus tell us how big a fraction of the available heavy flavor quarks binds to non-strange and strange heavy mesons, respectively. Using Fig. 8 the ratio γ_s/γ_q can be related to the s/S ratio. γ_q was chosen to conserve entropy during the hadronization process; see Fig. 6. In general, the heavy non-strange mesons yield decreases and the strange heavy meson yield increases with γ_s/γ_q. The yields D, B and D_s, B_s are summed over the excited states of D, B and D_s, B_s respectively – see Table 1 for the 'vertical tower' of resonances we have included.

Using γ_c, γ_s and γ_q at a given T (see Figs. 6, 7 and 10) we have now all the input required to compute the absolute and relative particle yields of all heavy hadrons that we can consider within the grand canonical phase space. When we consider the chemical equilibrium case, we naturally use $\gamma_s = \gamma_q = 1$.

In Fig. 13 we consider the yields shown in Fig. 12 as a function of the hadronization temperature. The dashed blue and green lines were obtained for the chemical equilibrium yields of D and D_s, respectively. The extreme upper and lower lines are for the fractional D and D_s yields with $s/S = 0.03$ (dot marked, blue and green lines, respectively), while the central lines are for $s/S = 0.04$ (solid, blue and green lines). Also we show the fractional yields for the maximal possible value $\gamma_q \to \gamma_q^{\mathrm{cr}}$; see Fig. 6 for $\gamma_q^{\mathrm{cr}}(T)$ (dash-dot lines) and (37).

We note that there is considerable symmetry at fixed T between the fractional yields of charm and bottom mesons, for the same condition of s/S. The chemical equilibrium results show a significant difference between the strange and non-strange heavy mesons. In the case of chemical equilibrium, for the very wide range of hadronization temperatures considered, $D_s/N_c \simeq B_s/N_b \simeq 0.2$ are nearly constant. A significant deviation from this result would suggest the presence of chemical non-equilibrium mechanisms for the heavy flavor meson production.

The yields of D_s/N_c and B_s/N_b are very similar, and similarly for D/N_c and B/N_b. Thus the relative yield of ei-

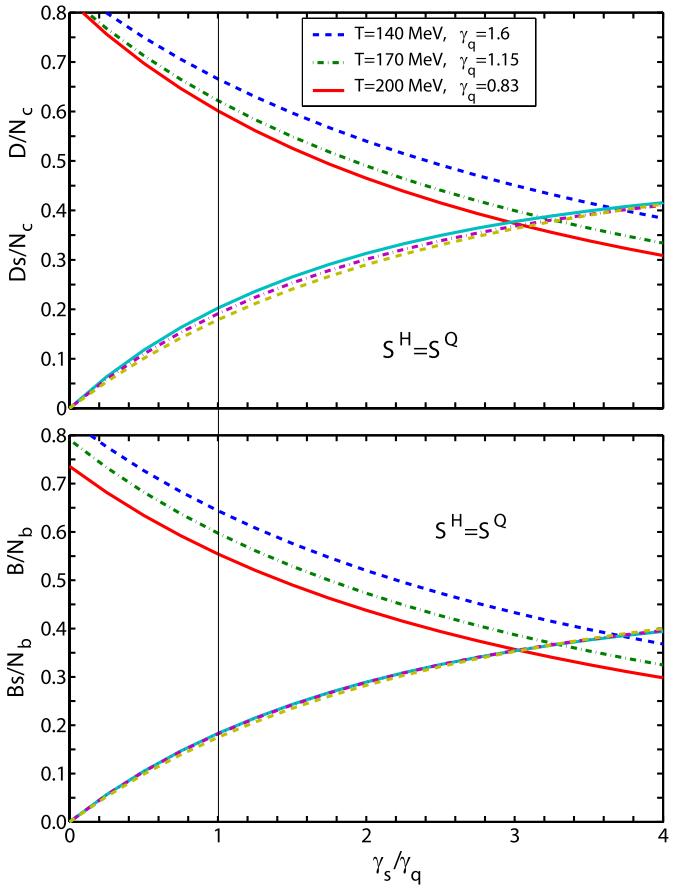

Fig. 12. *Upper panel*: fractional charm meson yield, and *lower panel*: the fractional bottom meson yields as a function of the γ_s/γ_q ratio for a fixed hadronization temperature T. The *upper lines* in each panel are for $D(B)$ mesons, the *solid line* is for $T = 200\,\mathrm{MeV}$, $\gamma_q = 1.1$, the *dashed line* is for $T = 170\,\mathrm{MeV}$, $\gamma_q = 1.15$ and the *dash-dot line* is for $T = 140\,\mathrm{MeV}$, $\gamma_q = 0.83$ ($S^{\mathrm{H}} = S^{\mathrm{Q}}$)

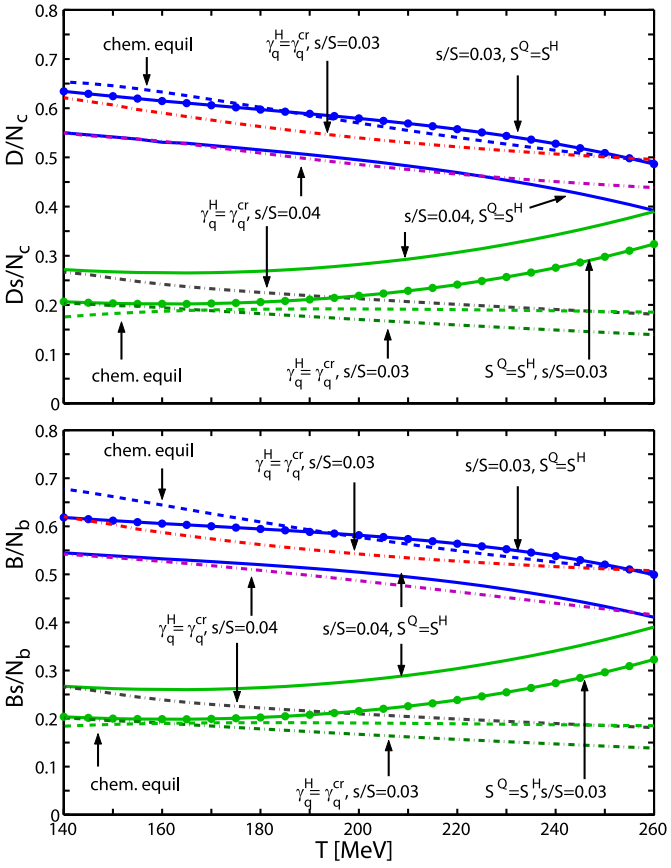

Fig. 13. *Upper panel*: fractional charm meson yield, and *lower panel*: fractional bottom meson yields. Equilibrium (*dashed lines*) and non-equilibrium for $s/S = 0.03$ (*point marked solid line*) and $s/S = 0.04$ (*solid line*) for D/N_c (*blue lines*, *upper panel*); D_s/N_c (*green lines*, *upper panel*); for D/N_c and D_s/N_c with $s/S = 0.03$ and $s/S = 0.04$ for $\gamma_q = \gamma_q^{\mathrm{cr}}$ (*dash-dotted lines*); B/N_b (*solid line*, *lower panel*); and B_s/N_b (*point marked solid line*, *lower panel*), for B/N_b and B_s/N_b with $s/S = 0.03$ and $s/S = 0.04$ for $\gamma_q = \gamma_q^{\mathrm{cr}}$ (*dash-dot lines*); as a function of T

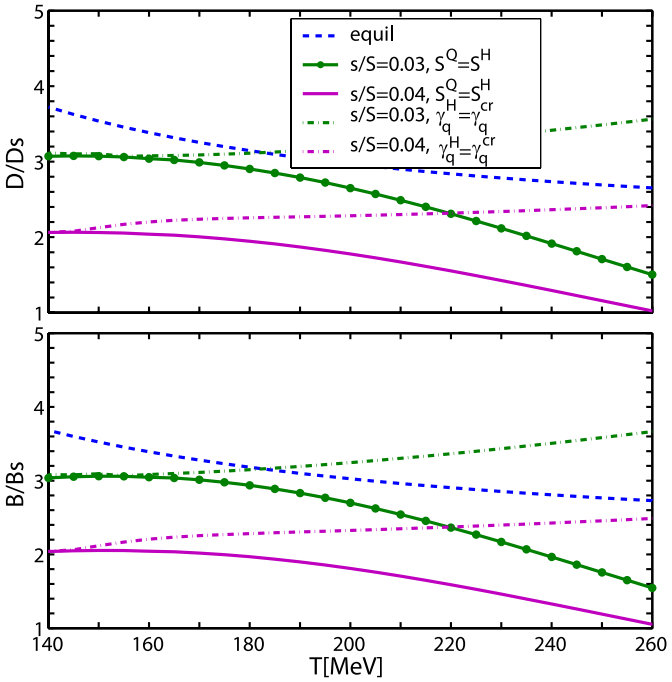

Fig. 14. The ratios D/D_s (*upper panel*) and B/B_s (*lower panel*) are shown as a function of T for different s/S ratios and in chemical equilibrium. The *solid line* is for $s/S = 0.04$, the *dash-dot line* is for $s/S = 0.03$, and the *dashed line* is for $\gamma_s^{\rm H} = \gamma_s^{\rm H} = 1$

ther of these mesons measures the relative yield of charm to bottom participating in the statistical hadronization process:

$$\frac{D_s}{B_s} \simeq \frac{D}{B} = \frac{N_c}{N_b}\,. \tag{49}$$

This is a very precise result, which somewhat depends on the tower of resonances included, and thus in particular on the symmetry in the heavy quark spectra between the charm and bottom states that we imposed.

It is useful to reconsider here the ratio D/D_s (B/B_s) which is proportional to γ_q/γ_s; see Fig. 1 for D_s/D presented as a function of γ_s/γ_q. We consider this ratio now as a function of T, the upper panel in Fig. 14 is for charm, the lower for bottom. We see that there is considerable symmetry in the relative yields between charm and bottom mesons, with upper and lower panels looking quasi-identical. Except for accidental values of T where the equilibrium results (blue, dashed lines) cross the fixed s/S results, there is considerable deviation in these ratios expected from chemical equilibrium. For LHC with $s/S = 0.04$, this ratio is always noticeably smaller than in chemical equilibrium (the solid purple line is for $S^{\rm Q} = S^{\rm H}$ and the purple dash-dot line is for $\gamma_q = \gamma_q^{\rm cr}$). Even for RHIC-like conditions with $s/S = 0.03$, this ratio is smaller than in chemical equilibrium for all temperatures when entropy conservation in hadronization is assumed, $S^{\rm Q} = S^{\rm H}$ (dot marked solid, green line).

6.3 Heavy baryon yields

As was the case when comparing charm to bottom mesons we also establish a symmetric set of charm and bottom baryons, shown in Table 4. Many of the bottom baryons are

Table 4. The charm and bottom baryon states considered. States in parentheses are not known experimentally and have been adopted from a theoretical source [35]

Hadron	M [GeV]	$Q: c, b$	Hadron	M [GeV]	g
$\Lambda_c^+(1/2^+)$	2.285	udQ	$\Lambda_b 0(1/2^+)$	5.624	2
$\Lambda_c^+(1/2^-)$	2.593	udQ	$\Lambda_b 0(1/2^-)$	(6.00)	2
$\Lambda_c^+(3/2^-)$	2.627	udQ	$\Lambda_b 0(1/2^-)$	(6.00)	2
$\Sigma_c^+(1/2^+)$	2.452	qqQ	$\Sigma_b^0(1/2^+)$	(5.77)	6
$\Sigma_c^*(3/2^+)$	2.519	qqQ	$\Sigma_b^{0*}(3/2^+)$	(5.78)	12
$\Xi_c(1/2^+)$	2.470	qsQ	$\Xi_b(1/2^+)$	(5.76)	4
$\Xi_c^{'}(1/2^+)$	2.574	qsQ	$\Xi_b^{'}(1/2^+)$	(5.90)	4
$\Xi_c(3/2^+)$	2.645	qsQ	$\Xi_b^{'}(3/2^+)$	(5.90)	8
$\Omega_c(1/2^+)$	2.700	ssQ	$\Omega_b(1/2^+)$	(6.00)	2
$\Omega_c(3/2^+)$	(2.70)	ssQ	$\Omega_b(3/2^+)$	(6.00)	4

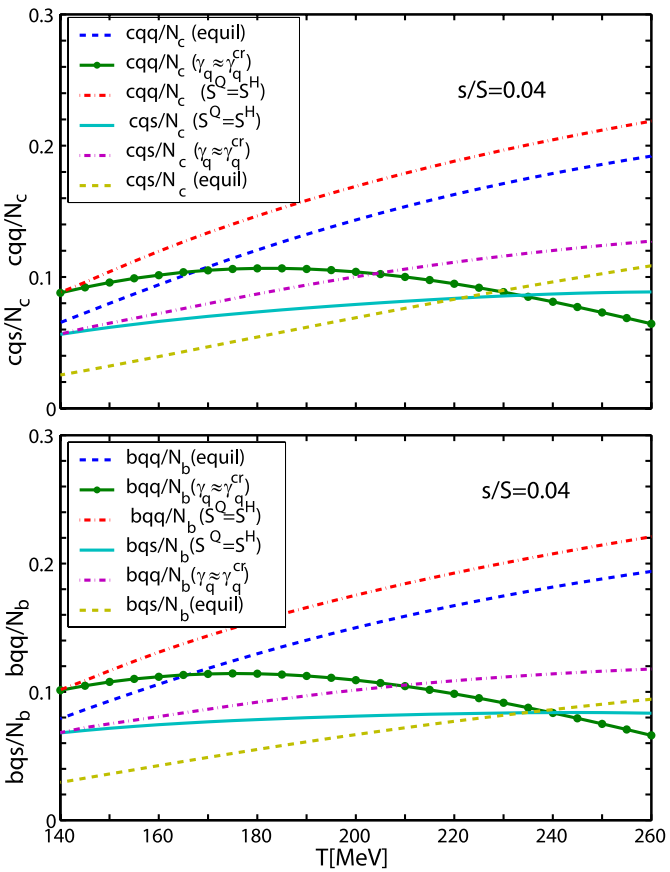

Fig. 15. Equilibrium (*dashed lines*), $s/S = 0.04$, $S^{\rm Q} = S^{\rm H}$ (*solid lines*), $s/S = 0.04$, $\gamma_q = \gamma_q^{\rm cr}$, (the *upper panel*) *upper lines* for each type are for ratio $(\Lambda_c + \Sigma_c)/N_c$ and *lower lines* are for Ξ_c/N_c (*upper panel*) and (*lower panel*) *upper lines* of each type are for $(\Lambda_b + \Sigma_b)/N_c$ and *lower lines* are for Ξ_b/N_b as functions of T

the result of theoretical studies, and we include that many states to be sure that both charm and bottom are consider in perfect symmetry to each other. In Fig. 15 (upper panel) we show the hadronization temperature dependencies of the yields of the baryons with one charm quark normalized to the charm multiplicity N_c. We show separately the yields of the baryons without the strange quark $(\Lambda_c + \Sigma_c)/N_c$, and with one strange quark $S = 1$ (Ξ_c/N_c). We show the two cases for $s/S = 0.04$ with conserved entropy at hadronization, $S^{\rm Q} = S^{\rm H}$ (solid lines), and with maximum possible entropy value, $\gamma_q = \gamma_q^{\rm cr}$ (dash-dot lines). The chemical equilibrium case $\gamma_q = \gamma_s = 1$ is also shown (dashed lines). The upper lines of each type are for $(\Lambda_c + \Sigma_c)/N_c$, the lower lines are for Ξ_c/N_c. A similar result is presented for bottom baryons in the lower panel of Fig. 15. We note that the result for bottom baryons is more uncertain since most baryon masses entering are not experimentally verified.

We note that the results shown in Fig. 15 imply that under LHC conditions at least 15% of the heavy flavor can be bound in heavy baryons, but possibly 30%. For the large value $\gamma_q = \gamma_q^{\rm cr} > 1$ we see an increase in the $(\Lambda_c + \Sigma_c)/N_c$ yields compared to chemical equilibrium and especially compared to entropy conserved hadronization, $S^{\rm Q} = S^{\rm H}$. This is so since the yields are proportional to γ_q^2 and $\gamma_s\gamma_q$. This results in a relative suppression of D_s/N_c (see Fig. 13).

In Fig. 16 we show the ratio $cqq/cqs = (\Lambda_c + \Sigma_c)/\Xi_c$ as a function of γ_s/γ_q for $T = 200\,\text{MeV}$ (dash-dot line),

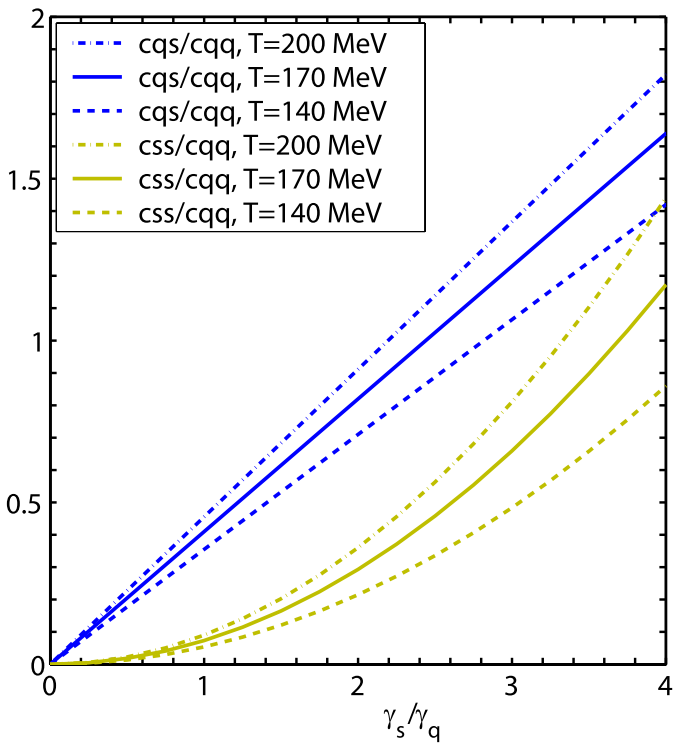

Fig. 16. The ratios $cqs/cqq = \Xi_c/(\Lambda_c + \Sigma_c)$ (*upper lines*) and $css/cqq = \Omega_c/(\Lambda_c + \Sigma_c)$ (*lower lines*) for $T = 200\,\text{MeV}$ (*dash-dot line*), $T = 170\,\text{MeV}$ (*solid line*) and $T = 140\,\text{MeV}$ (*dashed line*) as functions of γ_s/γ_q

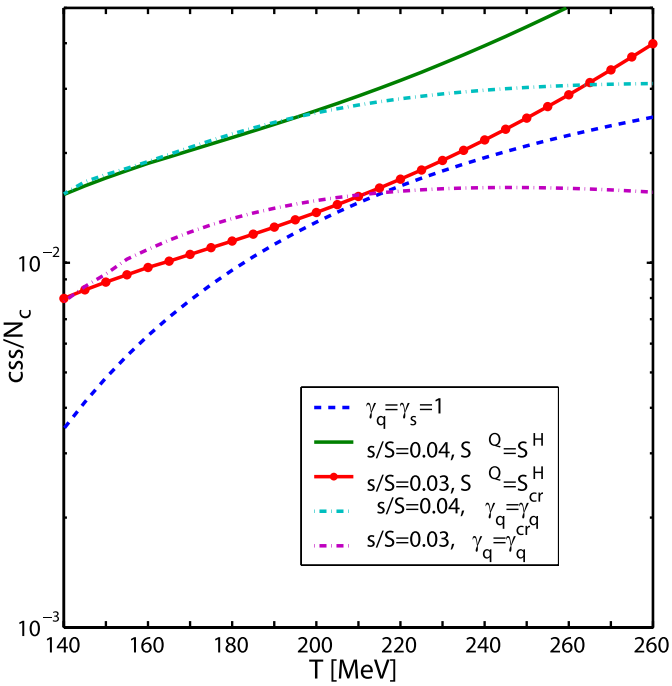

Fig. 17. $\Omega_c(css)/N_c$ as a function of T: the *dashed line* for chemical equilibrium; the *solid lines* are for $S^{\rm Q} = S^{\rm H}$, the *dashed dotted lines* are for $\gamma_q = \gamma_q^{\rm cr}$: both for $s/S = 0.03$ and $s/S = 0.04$ (*upper lines*)

$T = 170\,\text{MeV}$ (solid line) and $T = 140\,\text{MeV}$ (dashed line). This dependence is linear; the slope depends only on the hadronization temperature T. The ratio γ_s/γ_q can be converted to the ratio s/S using Fig. 8.

The yield of multi-strange charm baryons, $\Omega_c(css)$ is, similar to the light multi-strange hadrons, much more sensitive to chemical non-equilibrium. In Fig. 17 we see a large increase in the fractional yield of $\Omega_c(css)/N_c$ for $s/S = 0.04$ and $S^{\rm Q} = S^{\rm H}$ (solid line) compared to the chemical equilibrium (dashed line) expectation for the entire range of hadronization temperatures considered. As expected, this yields an increase with T. This also means that a higher formation temperature can be invoked to explain an unusually high yield. We expect that at LHC more than one percent of the total charm yield will be found in the $\Omega_c(css)$ state.

6.4 Yields of hadrons with two heavy quarks

We consider the multi-heavy hadrons listed in Table 5. The yields we will compute are now more model dependent, since we cannot completely reduce the result; it either remains dependent on the reaction volume $\mathrm{d}V/\mathrm{d}y$ or on the total charm (bottom) yields $\mathrm{d}N/\mathrm{d}y$. For example, the yields of hadrons with two heavy quarks are approximately proportional to $1/(\mathrm{d}V/\mathrm{d}y)$, because $\gamma_{b,c}^{\rm H}$ for heavy quarks is proportional to $1/\mathrm{d}V/\mathrm{d}y$, see (45):

$$\frac{\mathrm{d}N_{\rm hid}}{\mathrm{d}y} \propto \gamma_c^{H\,2}\frac{\mathrm{d}V}{\mathrm{d}y} \propto \frac{1}{\mathrm{d}V/\mathrm{d}y}, \qquad (50)$$

Table 5. The hidden charm and multi-heavy hadron states considered. States in parentheses are not known experimentally

Hadron		Mass (GeV)	g
$\eta_c(1S)$	$c\bar{c}$	2.9779	1
$J/\Psi(1S)$	$c\bar{c}$	3.0970	3
$\chi_{c0}(1P)$	$c\bar{c}$	3.4152	1
$\chi_{c1}(1P)$	$c\bar{c}$	3.5106	3
$h_c(1P)$	$c\bar{c}$	3.526	3
$\chi_{c2}(1P)$	$c\bar{c}$	3.5563	5
$\eta_c(2S)$	$c\bar{c}$	3.638	1
$\psi(2S)$	$c\bar{c}$	3.686	3
ψ	$c\bar{c}$	3.770	3
$\chi_{c2}(2P)$	$c\bar{c}$	3.929	5
ψ	$c\bar{c}$	4.040	3
ψ	$c\bar{c}$	4.159	3
ψ	$c\bar{c}$	4.415	3
B_c	$b\bar{c}$	6.27	1
Ξ_{cc}	ccq	3.527	4
Ω_{cc}	ccs	(3.660)	2

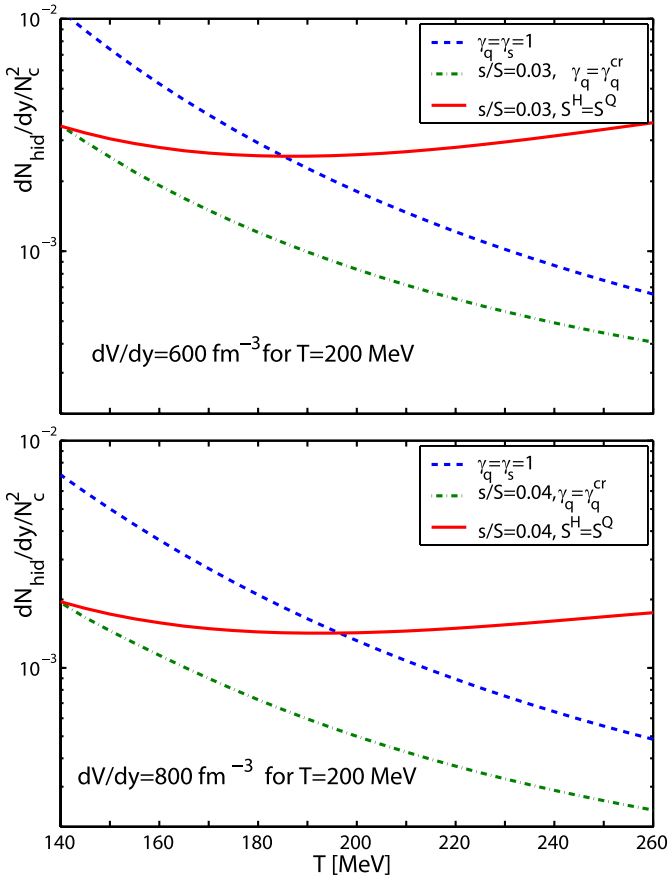

Fig. 18. The $c\bar{c}/N_c^2$ yields as a function of the hadronization temperature T, at $\mathrm{d}V/\mathrm{d}y = 600\,\mathrm{fm}^{-3}$ for $T = 200$ MeV, $s/S = 0.03$ (*upper panel*), $\mathrm{d}V/\mathrm{d}y = 800\,\mathrm{fm}^{-3}$ for $T = 200$ MeV, $s/S = 0.04$ (*lower panel*). The results shown are for $S^{\mathrm{Q}} = S^{\mathrm{H}}$ (*solid lines*), for $\gamma_q = \gamma_q^{\mathrm{cr}}$ (*dash-dot lines*), and for the chemical equilibrium case (*dashed lines*; s/S is not fixed)

$$\frac{\mathrm{d}N_{B_c}}{\mathrm{d}y} \propto \gamma_c^{\mathrm{H}}\gamma_b^{\mathrm{H}}\frac{\mathrm{d}V}{\mathrm{d}y} \propto \frac{1}{\mathrm{d}V/\mathrm{d}y}\,. \tag{51}$$

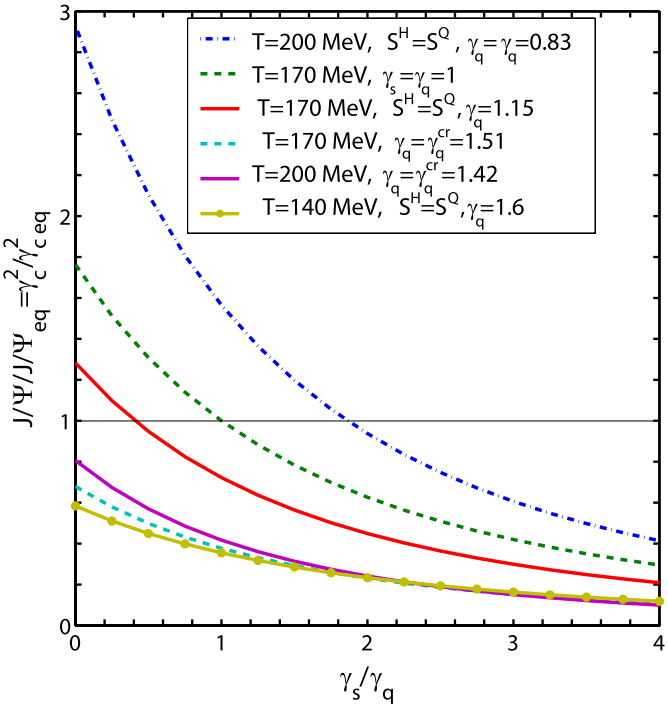

Fig. 19. The ratio $J/\Psi/J/\Psi_{\mathrm{eq}} = \gamma_c^2/\gamma_{c\,\mathrm{eq}}^2$ as a function of $\gamma_s^{\mathrm{H}}/\gamma_q^{\mathrm{H}}$ at a fixed value of γ_q^{H} and if required, entropy conservation. Shown are $T = 200$ MeV at $\gamma_q = 0.83$ (*dot-dash line*) and at $\gamma_q = \gamma_q^{\mathrm{cr}} = 1.42$ (*lower solid line* (*purple*)); $T = 170$ MeV at $\gamma_q = 1$ (*upper dashed line*) , at $\gamma_q = 1.15$, (*upper solid line* (*red*)), and at $\gamma_q = \gamma_q^{\mathrm{cr}} = 1.51$, (*lower dashed line*); and $T = 140$ MeV, $\gamma_q = 1.6$

Moreover, unlike the case for single heavy hadrons, the canonical correction to grand canonical phase space does not cancel out in these states, adding to the uncertainty.

Thus the result we present must be seen as a guide to the eye and demonstrating a principle. In Fig. 18 we show the yield of hidden charm $c\bar{c}$ mesons (see Table 5) normalized by the square of the charm multiplicity, N_c^2, as a function of the hadronization temperature T. We consider again the cases with $s/S = 0.03$ (upper panel) and $s/S = 0.04$ (lower panel); the solid line is for $S^{\mathrm{H}} = S^{\mathrm{Q}}$, the dot-dash line is for $\gamma_q = \gamma_q^{\mathrm{cr}}$, and the dot-dash line is for $\gamma_q = \gamma_q^{\mathrm{cr}}$. The chemical equilibrium $c\bar{c}$ mesons yields are shown (dashed lines on both panels) for two different values of $\mathrm{d}V/\mathrm{d}y = 600\,\mathrm{fm}^3$ for $T = 200$ MeV (upper panel) and $\mathrm{d}V/\mathrm{d}y = 800\,\mathrm{fm}^3$ for $T = 200$ MeV (lower panel).

The yield of the $c\bar{c}$ mesons is much smaller for $s/S = 0.04$ than in equilibrium for the same $\mathrm{d}V/\mathrm{d}y$ for a large range of hadronization temperatures. For $s/S = 0.03$ the effect is similar, but the suppression is not as pronounced. For $\gamma_q = \gamma_q^{\mathrm{cr}}$ suppression, the yield of the hidden charm particles is always smaller than the equilibrium value. This suppression occurs due to competition with the yield of strange heavy mesons, and also, when $\gamma_q > 1$, with heavy baryons with two light quarks. The enhanced yield of D and D_s and heavy baryons in effect depletes the pool of available charm quark pairs, and fewer hidden charm $c\bar{c}$

mesons are formed. For particles with two heavy quarks the effect is larger than for hadrons with one heavy quark and light quark(s).

In Fig. 19 we compare the J/Ψ yield to the chemical equilibrium yield $\Psi/J/\Psi_{\rm eq}$ as a function of $\gamma_s^{\rm H}/\gamma_q^{\rm H}$; each line is at a fixed value of $\gamma_q^{\rm H}$. This ratio is

$$\frac{J/\Psi}{J/\Psi_{\rm eq}} = \frac{N_{\rm hid}}{N_{\rm hid\,eq}} = \frac{\gamma_c^2}{\gamma_{c\,\rm eq}^2}\,. \qquad (52)$$

$J/\Psi/J/\Psi_{\rm eq}$ always decreases when γ_s/γ_q increases. For $\gamma_q = \gamma_{cr}$, $J/\Psi/J/\Psi_{\rm eq}$ is smaller than unity, even when $\gamma_s \to 0$, because of the large phase space occupancy of the light quarks. We have $J/\Psi/J/\Psi_{\rm eq} > 1$ for small γ_q and small γ_s/γ_q.

Considering the product of the J/Ψ and ϕ yields normalized by N_c^2, we eliminate nearly all the uncertainty about the yield of charm and/or the hadronization volume. However, we tacitly assume that both J/Ψ and ϕ hadronize at the same temperature. In Fig. 20 we show $J/\Psi\phi/N_c^2$ as a function of γ_s/γ_q. There is a considerable difference to the ratio considered in Fig. 2. We see mainly a dependence on γ_s/γ_q. As before, see Sect. 3.2, J/Ψ is the sum of all states $c\bar{c}$ from Table 5 that can decay to J/Ψ. We show the results for $T = 200$ MeV (solid lines), $T = 170$ MeV (dashed line) and $T = 140$ MeV (dash-dot line). The γ_q, for each T, is fixed by the entropy conservation condition during hadronization (Fig. 6) (thick lines) or by $\gamma_q = \gamma_q^{\rm cr}$ (thin lines). For $T = 140$ MeV, these lines coincide. $T = 170$ MeV, the $\gamma_q = 1$ case is also shown (solid line with dot markers). The s/S values that correspond to a given ratio γ_s/γ_q can be found in Fig. 8. Figure 20 shows that, despite the yield $\phi/({\rm d}V/{\rm d}y)$ increasing as $(\gamma_s/\gamma_q)^2$, $J/\Psi\phi/N_c^2$ is increasing as γ_s/γ_q, considering compensation effects.

A similar situation as in Fig. 19 for hidden charm, arises for the B_c meson yield, see Fig. 21, where the ratio B_c/N_cN_b is shown as a function of the hadronization temperature T, for the same strangeness yield cases as discussed for the hidden charm meson yield. Despite the suppression in a strangeness-rich environment, the B_c meson yield continues to be larger than the yield of B_c produced in single NN collisions, where the scale yield is at the level of $\sim 10^{-5}$; see the cross sections for $b\bar{b}$ and B_c production in [11] and in [36], respectively.

In Fig. 22 we show the N_c^2 scaled yields of the ccq and ccs baryons as a function of temperature. The upper panel shows aside of the equilibrium case (dashed lines) the yields for $s/S = 0.04$ with $S^{\rm H} = S^{\rm Q}$ (solid lines) and with $\gamma_q = \gamma_q^{\rm cr}$ (dash-dot line) for ${\rm d}V/{\rm d}y = 800\,{\rm fm}^{-3}$ for $T = 200$ MeV. The lower panel is for ${\rm d}V/{\rm d}y = 600\,{\rm fm}^{-3}$

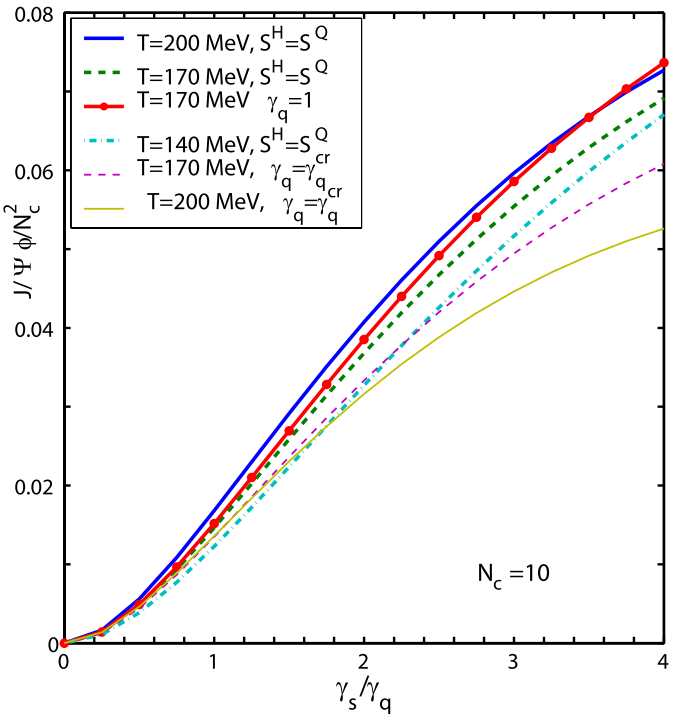

Fig. 20. The yields of the $J/\Psi\phi/N_c^2$ states as a function of the ratio γ_s/γ_q for $T = 200$ MeV, $S^{\rm Q} = S^{\rm H}$ (*solid line*) and $\gamma_q = \gamma_q^{\rm cr}$ (solid thin line), $T = 170$ MeV (*dashed line*), $\gamma_q = \gamma_q^{\rm cr}$ (*thin dashed line*) and $\gamma_q = 1$ (*solid line with dot marker*); for $T = 140$ MeV, $S^{\rm Q} = S^{\rm H}$ (*dash-dot line*)

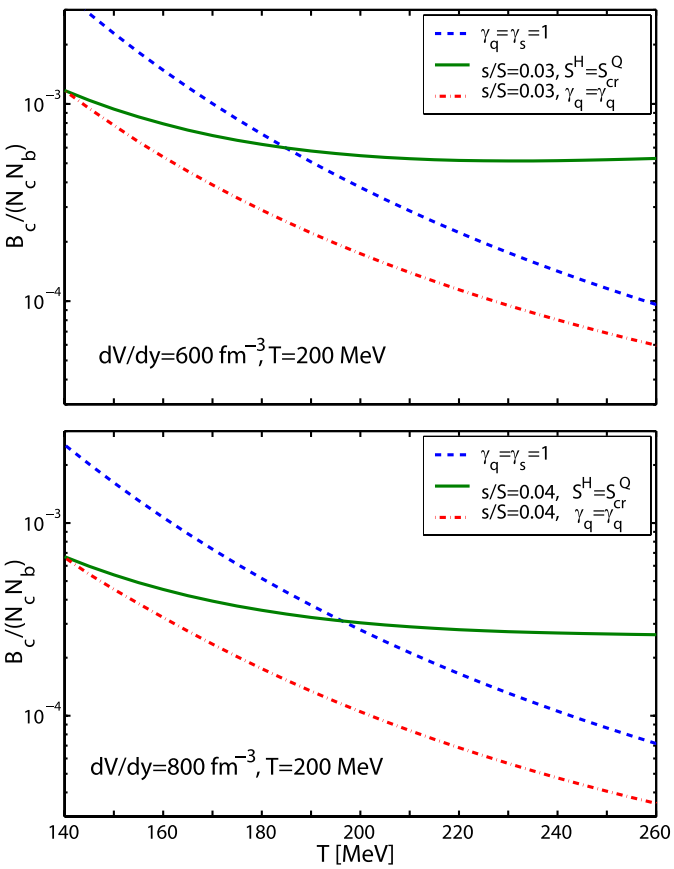

Fig. 21. The B_c mesons yields as a function of T for the chemical equilibrium case with ${\rm d}V/{\rm d}y = 600\,{\rm fm}^{-3}$ for $T = 200$ MeV (the *upper panel*, *dashed line*), for $s/S = 0.03$ with ${\rm d}V/{\rm d}y = 600\,{\rm fm}^{-3}$ for $T = 200$ MeV (the *upper panel*, *solid line*), for the chemical equilibrium case with ${\rm d}V/{\rm d}y = 800\,{\rm fm}^{-3}$ for $T = 200$ MeV (the *lower panel*, *dashed line*) for $s/S = 0.04$ ${\rm d}V/{\rm d}y = 800\,{\rm fm}^{-3}$ for $T = 200$ MeV (*lower panel*, *solid line*)

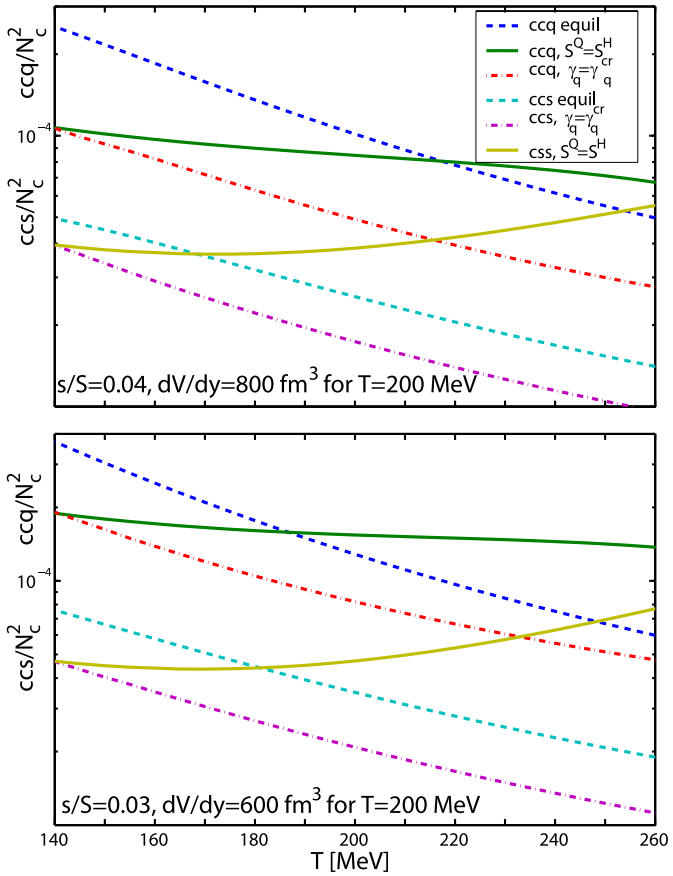

Fig. 22. The ccq/N_c^2 (*upper lines* in each panel) and ccs/N_c^2 (*lower lines* in each panel) baryon yields as a function of T. *Upper panel*: chemical equilibrium case with $\mathrm{d}V/\mathrm{d}y = 800\,\mathrm{fm}^{-3}$ for $T = 200\,\mathrm{MeV}$ (*dashed line*), $s/S = 0.04$ with $\mathrm{d}V/\mathrm{d}y = 800\,\mathrm{fm}^{-3}$ for $T = 200\,\mathrm{MeV}$: $S^{\mathrm{H}} = S^{\mathrm{Q}}$ (*solid line*) and $\gamma_q = \gamma_q^{\mathrm{cr}}$ (*dash-dot line*); and *lower panel*: chemical equilibrium case with $\mathrm{d}V/\mathrm{d}y = 600\,\mathrm{fm}^{-3}$ for $T = 200\,\mathrm{MeV}$ (*dashed line*), and $s/S = 0.03$ $S^{\mathrm{Q}} = S^{\mathrm{H}}$ (*solid line*) and $\gamma^q = \gamma_q^{\mathrm{cr}}$ (*dash-dot line*)

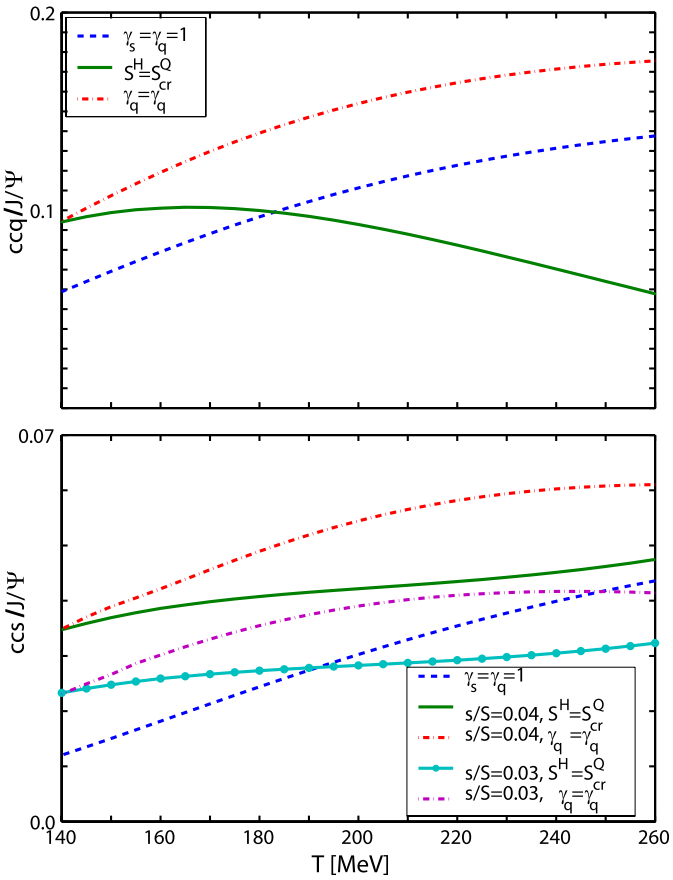

Fig. 23. The ratios $ccq/J/\Psi$ (*upper panel*) and $ccs/J/\Psi$ (*lower panel*) as a function of T. Upper panel: the chemical equilibrium case (*dashed line*), $S^{\mathrm{H}} = S^{\mathrm{Q}}$ (*solid line*) and $\gamma_q = \gamma_q^{\mathrm{cr}}$ (*dashed-dot line*), and *lower panel*: the chemical equilibrium case with (*dashed line*), $s/S = 0.04$: $S^{\mathrm{Q}} = S^{\mathrm{H}}$ (*solid line with dot marker*) and $\gamma_q = \gamma_q^{\mathrm{cr}}$ (*thin dash-dot line*); $s/S = 0.03$ (*solid line*) and $\gamma_q = \gamma_q^{\mathrm{cr}}$ (*thin dash-dot line*)

and $s/S = 0.03$. For the ccq baryons the chemical non-equilibrium suppression effect is similar to what we saw for the $c\bar{c}$ and B_c mesons. The equilibrium yield is much larger than the non-equilibrium one for $T < 230\,\mathrm{MeV}$ when $s/S = 0.04$ and $S^{\mathrm{H}} = S^{\mathrm{Q}}$, and for $T < 190\,\mathrm{MeV}$ when $s/S = 0.03$ and $S^{\mathrm{H}} = S^{\mathrm{Q}}$. In the case of $\gamma_q = \gamma_q^{\mathrm{cr}}$, the yield of ccq is always smaller than at equilibrium. The yield of the ccs baryons has a similar suppression, but it becomes larger than equilibrium for smaller temperatures and the yield enhancement for higher T is larger for $S^{\mathrm{H}} = S^{\mathrm{Q}}$ than in the case of ccq, because of the large number of strange quarks.

In Fig. 23 we show the ratios $ccq/J/\Psi$ (upper panel) and $ccs/J/\Psi$ (lower panel) as a function of hadronization temperature. These ratios do not depend on $\mathrm{d}V/\mathrm{d}y$. $ccq/J/\Psi \propto \gamma_q$ does not depend on s/S. For the ratio $ccq/J/\Psi$, we show three cases: chemical equilibrium, $\gamma_s = \gamma_q = 1$ (dashed line), $S^{\mathrm{H}} = S^{\mathrm{Q}}$ (solid line) and $\gamma_q = \gamma_q^{\mathrm{cr}}$ (dash-dot line). For $ccs/J/\Psi$ ($ccq/J/\Psi \propto \gamma_s$), we show the chemical equilibrium case (dashed line), $s/S = 0.04$: $S^{\mathrm{H}} = S^{\mathrm{Q}}$ (solid line with point marker) and $\gamma_q = \gamma_q^{\mathrm{cr}}$ (thin dash-dot line); $s/S = 0.03$: $S^{\mathrm{H}} = S^{\mathrm{Q}}$ (solid line) and $\gamma_q = \gamma_q^{\mathrm{cr}}$ (thin dash-dot line). The overall yields of double charm (strange and non-strange) baryons and antibaryons is clearly larger than the yield of J/Ψ.

7 Conclusions

We have considered here in some detail the abundances of the heavy flavor hadrons within the statistical hadronization model. While we compare the yields to the expectations based on the chemical equilibrium yields of the light and strange quark pairs, we present results based on the hypothesis that the QGP entropy and QGP flavor yields determine the values of the phase space occupancy γ_i^{H} $i = q, s, c, b$, which are of direct interest in the study of the heavy hadron yields.

For the highest energy heavy-ion collisions the range of values discussed in the literature is $1 \leq \gamma_q^{\mathrm{H}} \leq 1.65$ and $0.7 \leq \gamma_s^{\mathrm{H}}/\gamma_q^{\mathrm{H}} \leq 1.5$. However, values of γ_c^{H} and γ_b^{H} that are

much larger than unity arise. This is due to the need to describe the large primary parton based production, and considering that the chemical equilibrium yields are suppressed by the factor $\exp(-m/T)$.

Our work is based on the grand canonical treatment of phase space. This approach is valid for the charm hadron production at LHC, since the canonical corrections, as we have discussed, are not material. On the other hand, even at LHC the much smaller yields of the heavy bottom hadrons are subject to canonical suppression. The value of the parameter $\gamma_b^{\rm H}$ obtained at a fixed bottom yield N_b, using either the canonical or the grand canonical methods, are different, see e.g. (15) in [37]. Namely, to obtain a given yield N_b in the canonical approach, a greater value of $\gamma_b^{\rm H}$ is needed in order to compensate for the canonical suppression effect. However, for any individual single-b hadron, the relative yields, e.g. B/B_s, do not depend on $\gamma_b^{\rm H}$ and thus such ratios are not influenced by a canonical suppression. Moreover, as long as the yield of single-b hadrons dominates the total bottom yield, $N_b \simeq B + B_s + \Lambda_b + \ldots$, also the N_b scaled yields of hadrons comprising one b quark, i.e. ratios such as B/N_b, B_s/N_b, B_c/N_b, etc., are not sensitive to the value of $\gamma_b^{\rm H}$ and can be obtained within either the canonical or the grand canonical method. On the other hand, for $b\bar{b}$ mesons and multi-b baryons the canonical effects should be considered. The study of the yields of these particles is thus postponed.

We address here in particular how the yields of the heavy hadrons are influenced by $\gamma_s^{\rm H}/\gamma_q^{\rm H} \neq 1$ and $\gamma_q \neq 1$. The actual values of $\gamma^{\rm H} s/\gamma_q^{\rm H}$ that we use are related to the strangeness per entropy yield s/S established in the QGP phase. Because the final value of s/S is established well before hadronization, and the properties of the hadron phase space are well understood, the resulting $\gamma_s^{\rm H}/\gamma_q^{\rm H}$ are well defined and turn out to be quite different from unity in the range of temperatures in which we expect particle freeze-out to occur. We consider in some detail the effect of QGP hadronization on the values of $\gamma_s^{\rm H}$ and $\gamma_q^{\rm H}$.

One of the first results we present (Fig. 2) allows for a test of the statistical hadronization model for a heavy flavor: we show that the yield ratio $c\bar{c}s\bar{s}/(c\bar{s}\bar{c}s)$ is nearly independent of temperature and it is also nearly constant when the ϕ is allowed to freeze out later (Fig. 3), provided that the condition of production is at the same value for the strangeness per entropy s/S.

We studied in depth how the (relative) yields of strange and non-strange charm mesons vary with strangeness content. For a chemically equilibrated QGP source, there is a considerable shift of the yield from non-strange D to the strange D_s for $s/S = 0.04$ as expected at LHC. The expected fractional yield $D_s/N_c \simeq B_s/N_b \simeq 0.2$ when one assumes $\gamma^{\rm H} s = \gamma_q^{\rm H} = 1$, and the expected enhancement of the strange heavy mesons is at the level of 30% when $s/S = 0.04$, and greater when a greater strangeness yield is available.

A consequence of this result is that we find a relative suppression of the multi-heavy hadrons, except when they contain strangeness. The somewhat ironic situation is that while a charm QGP yield higher beyond chemical equilibrium enhances the production of $c\bar{c}$ states, enhanced light quarks and strangeness multiplicity beyond chemical equilibrium suppresses this almost by as much. This new phenomenon adds to the complexity of the interpretation of the hidden charm meson yield. On the other hand, the yield of $c\bar{c}/N_c^2 \simeq 2\cdot 10^{-3}$ is found to be almost independent on the hadronization temperature in the case that conserves entropy at hadronization. We do not know exactly the equation of state in QGP, and so the value of γ_q that is needed to conserve the entropy may be different. If γ_q is larger for higher temperatures, the suppression of $c\bar{c}$ is larger for a fixed s/S. The same result is found for $B_c \approx 5\text{–}6\times 10^{-4} N_c N_b$; that yield remains considerably larger (by a factor 10–100) compared to the scaled yield in single nucleon–nucleon collisions.

We have shown that the study of heavy flavor hadrons will provide important information on the nature and properties of the QGP hadronization. The yield of the B_c ($b\bar{c}$) mesons remains enhanced, while the hidden charm $c\bar{c}$ states encounter another suppression mechanism, compensating for the greatly enhanced production due to the large charm yield at LHC.

Acknowledgements. Work supported by a grant from the U.S. Department of Energy DE-FG02-04ER4131.

References

1. K. Geiger, Phys. Rev. D **48**, 4129 (1993)
2. M. Cacciari, P. Nason, R. Vogt, Phys. Rev. Lett. **95**, 122 001 (2005) [arXiv:hep-ph/0502203]
3. H. van Hees, R. Rapp, Phys. Rev. C **71**, 034 907 (2005) [arXiv:nucl-th/0412015]
4. M. Schroedter, R.L. Thews, J. Rafelski, Phys. Rev. C **62**, 024 905 (2000) [arXiv:hep-ph/0004041]
5. F. Becattini, Phys. Rev. Lett. **95**, 022 301 (2005) [arXiv:hep-ph/0503239]
6. R.L. Thews, Eur. Phys. J. C **43**, 97 (2005) [arXiv:hep-ph/0504226]
7. I. Kuznetsova, J. Rafelski, J. Phys. G **32**, S499 (2006) [arXiv:hep-ph/0605307]
8. P. Koch, B. Muller, J. Rafelski, Phys. Rep. **142**, 167 (1986)
9. A. Andronic, P. Braun-Munzinger, K. Redlich, J. Stachel, Phys. Lett. B **571**, 36 (2003) [arXiv:nucl-th/0303036]
10. M. Bedjidian et al., Hard probes in heavy-ion collisions at the LHC: Heavy flavour physics, arXiv:hep-ph/0311048, in: M. Mangano, H. Satz, U. Wiedermann, Hard probes in heavy-ion collisions at the LHC, pp. 247–346, CERN-2004-009, Yellow Report, http://doc.cern.ch/cernrep/2004/2004-009/2004-009.html
11. K. Anikeev et al., B physics at the Tevatron: Run II and beyond, arXiv:hep-ph/0201071, SLAC-REPRINT-2001-056, FERMILAB-PUB-01-197, December 2001. pp. 583 Workshop on B Physics at the Tevatron: Run II and Beyond, Batavia, Illinois, 24–26 February 2000
12. J. Letessier, J. Rafelski, Phys. Rev. C **75**, 014 905 (2007) [arXiv:nucl-th/0602047]
13. E. Fermi, Prog. Theor. Phys. **5**, 570 (1950)

14. R. Hagedorn, How We Got To QCD Matter From The Hadron Side By Trial And Error, CERN-TH-3918/84 Invited talk given at Quark Matter 1984, 4th Int. Conf. on Ultrarelativistic Nucleus-Nucleus Collisions, Helsinki, Finland, June 17–21, 1984 ed. by K. Kajantie, Springer, Lecture Notes in Physics, 221, pp. 53–76
15. D0 Collaboration, E. Cheu, Int. J. Mod. Phys. A **20**, 3664 (2005)
16. J.D. Bjorken, Phys. Rev. D **27**, 140 (1983)
17. J.I. Kapusta, Nucl. Phys. B **148**, 461 (1979)
18. S. Hamieh, J. Letessier, J. Rafelski, Phys. Rev. C **62**, 064 901 (2000) [arXiv:hep-ph/0006085]
19. J.I. Kapusta, C. Gale, Finite-Temperature Field Theory: Principles and Applications, in: Cambridge Monographs on Mathematical Physics (Cambridge University Press, Cambridge, New York, 2006)
20. J. Letessier, J. Rafelski, Phys. Rev. C **67**, 031 902 (2003) [arXiv:hep-ph/0301099]
21. J. Rafelski, J. Letessier, Nucl. Phys. A **702**, 304 (2002) [arXiv:hep-ph/0112027]
22. G. Torrieri, S. Steinke, W. Broniowski, W. Florkowski, J. Letessier, J. Rafelski, (SHARE 1) Comput. Phys. Commun. **167**, 229 (2005) [arXiv:nucl-th/0404083]
23. G. Torrieri, S. Jeon, J. Letessier, J. Rafelski, (SHARE 2) Comput. Phys. Commun. **175**, 635 (2006) [arXiv:nucl-th/0603026]
24. J. Letessier, A. Tounsi, U.W. Heinz, J. Sollfrank, J. Rafelski, Phys. Rev. Lett. **70**, 3530 (1993) [arXiv:hep-ph/9711349]
25. J. Letessier, A. Tounsi, U.W. Heinz, J. Sollfrank, J. Rafelski, Phys. Rev. D **51**, 3408 (1995) [arXiv:hep-ph/9212210]
26. J.I. Kapusta, A. Mekjian, Phys. Rev. D **33**, 1304 (1986)
27. J. Letessier, J. Rafelski, A. Tounsi, Phys. Lett. B **323**, 393 (1994) [arXiv:hep-ph/9711345]
28. A. Wroblewski, Acta Phys. Pol. B **16**, 379 (1985)
29. R.V. Gavai, S. Gupta, Phys. Rev. D **65**, 094 515 (2002) [arXiv:hep-lat/0202006]
30. R.V. Gavai, S. Gupta, J. Phys. G **32**, S275 (2006) [arXiv:hep-ph/0605254]
31. R.V. Gavai, S. Gupta, Eur. Phys. J. C **43**, 31 (2005) [arXiv:hep-ph/0502198]
32. J. Rafelski, J. Letessier, Eur. Phys. J. A **29**, 107 (2006) [arXiv:nucl-th/0511016]
33. T. Matsuki, T. Morii, Phys. Rev. D **56**, 5646 (1997)
34. T. Matsuki, T. Morii, Austral. J. Phys. **50**, 163 (1997) [arXiv:hep-ph/9702366]
35. C. Albertus, J.E. Amaro, E. Hernandez, J. Nieves, Nucl. Phys. A **740**, 333 (2004) [arXiv:nucl-th/0311100]
36. C.H. Chang, X.G. Wu, Eur. Phys. J. C **38**, 267 (2004) [arXiv:hep-ph/0309121]
37. J. Rafelski, J. Letessier, J. Phys. G **28**, 1819 (2002) [arXiv:hep-ph/0112151]